ACS Sustainable Chemistry & Engineering

pubs.acs.org/journal/ascecg

Research Article

Process Simulations of High-Purity and Renewable Clean H_2 Production by Sorption Enhanced Steam Reforming of Biogas

Alma Capa, Yongliang Yan, Fernando Rubiera, Covadonga Pevida,* María Victoria Gil,* and Peter T. Clough

Cite This: *ACS Sustainable Chem. Eng.* 2023, 11, 4759−4775

Read Online

ACCESS | Metrics & More | Article Recommendations | Supporting Information

ABSTRACT: Renewable clean H_2 has a very promising potential for the decarbonization of energy systems. Sorption enhanced steam reforming (SESR) is a novel process that combines the steam reforming reaction and the simultaneous CO_2 removal by a solid sorbent, such as CaO, which significantly enhances hydrogen generation, enabling high-purity H_2 production. The CO_2 sorption reaction (carbonation) is exothermic, but the sorbent regeneration by calcination is highly endothermic, which requires extra energy. Biogas is one of the available carbon-neutral renewable H_2 production sources. It can be especially relevant for the energy integration of the SESR process since, due to the exothermic sorption reaction, the CO_2 contained in the biogas provides extra heat to the system, which can help to balance the energy requirements of the process. This work studies different process configurations for the energy integration of the SESR process of biogas for high-purity renewable H_2 production: (1) SESR with sorbent regeneration using a portion of the produced H_2 (SESR+REG_H_2), (2) SESR with sorbent regeneration using biogas (SESR+REG_BG), and (3) SESR with sorbent regeneration using biogas and adding a pressure swing adsorption (PSA) unit for hydrogen purification (SESR+REG_BG+PSA). When using biogas as fuel (Cases 2 and 3), these configurations were studied using air and oxy-fuel combustion atmospheres in the sorbent regeneration step, resulting in five case studies. A thermodynamic approach for process modeling can provide the optimal process operating conditions and configurations that maximize the energy efficiency of the process, which are the basis for subsequent optimization of the process at the practical level needed to scale up this technology. For this purpose, process simulations were performed using a steady-state plant model developed in Aspen Plus, incorporating a complex heat exchanger network (HEN) to optimize heat integration. A comprehensive parametric study assessed the effects of biogas composition, temperature, pressure, and steam to methane (S/CH_4) ratio on the process performance represented by the selected key performance indicators, i.e., H_2 purity, H_2 yield, CH_4 conversion, cold gas efficiency (CGE), net efficiency (NE), fuel consumption for the sorbent regeneration step, and CO_2 capture efficiency. H_2 with a purity of 98.5 vol % and a CGE of 75.7% with zero carbon emissions can be achieved. When adding a PSA unit, nearly 100% H_2 purity and CO_2 capture efficiency were achieved with a CGE of 77.3%. The use of oxy-fuel combustion during regeneration lowered the net efficiency of the process by 2.3% points (since it requires an air separation unit) but allowed the process to achieve negative carbon emissions.

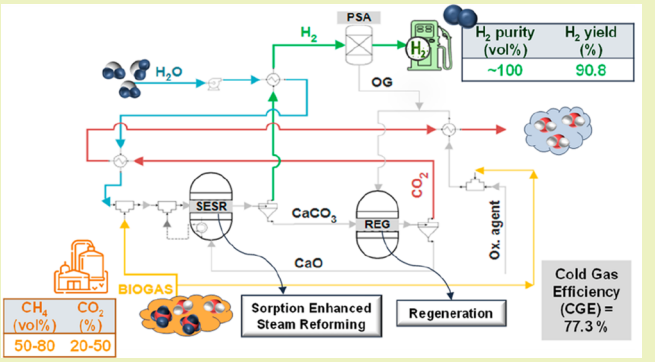

KEYWORDS: *Biogas, CH_4/CO_2 composition, Hydrogen, Sorption enhanced steam reforming, Process simulation, CO_2 capture*

INTRODUCTION

Hydrogen is a versatile feedstock and an attractive energy carrier, positioned as one of the main pillars for the imminent energy transition toward climate change mitigation.[1] However, most of the produced hydrogen comes from fossil resources, either by steam reforming (SR) of methane/natural gas and oil/naphtha or from coal gasification without CO_2 capture.[2] For instance, ~90 Mt of H_2 was used in 2020 and around 80% was produced from fossil fuels (all the remaining came from residual gases), mostly unabated, which resulted in 900 Mt CO_2 emitted in the production of H_2.[3] The conventional SR process usually performs at high temperatures (700−1000 °C) and pressures (15−40 bar). In this process, the endothermic reforming reaction takes place in high-alloy reformer tubes where the catalyst is placed, which in most cases is Ni based. The reformer operates using typical steam to carbon (S/C) ratios from 2 to 6, and external gas burners heat the reformer

Received: December 8, 2022
Revised: February 27, 2023
Published: March 11, 2023

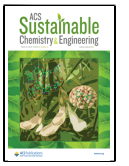

tubes.[4,5] The process is endothermic and renders low H_2 yield and purity prompting the need for a series of high- and low-temperature water−gas shift (WGS) reactors and hydrogen purification units.

Sorption enhanced steam reforming (SESR) is emerging as a novel intensification process of the conventional SR technology.[6] In the case of the sorption enhanced steam methane reforming (SESMR), in situ CO_2 capture by a solid sorbent material, such as CaO, is performed by eq 1, together with steam methane reforming (SMR, eq 2) and WGS (eq 3) reactions. Due to the addition of the sorbent, the equilibrium of SMR and WGS is shifted toward the forward direction according to Le Chatelier's principle, favoring not solely the increase in the H_2 productivity but also the H_2 purity and reactants conversion.[7] In addition, the overall reaction of SESMR is slightly exothermic (eq 4), which could entail a reduction in the external utility demand (i.e., external gas burners that are necessary for conventional SR reactors). Regeneration of the sorbent occurs through the reverse carbonation reaction of CaO (reverse of eq 1).

$$CaO_{(s)} + CO_2 \leftrightarrow CaCO_{3(s)} \quad \Delta H_r^0 = -178\,kJ\,mol^{-1} \tag{1}$$

$$CH_4 + H_2O \leftrightarrow CO + 3H_2 \quad \Delta H_r^0 = +206\,kJ\,mol^{-1} \tag{2}$$

$$CO + H_2O \leftrightarrow CO_2 + H_2 \quad \Delta H_r^0 = -41\,kJ\,mol^{-1} \tag{3}$$

$$CH_4 + 2H_2O + CaO_{(s)} \rightarrow 4H_2 + CaCO_{3(s)} \quad \Delta H_r^0 = -13\,kJ\,mol^{-1} \tag{4}$$

Hydrogen gains higher interest when produced using low- or zero-carbon energy sources,[1] which is imperative to fulfill climate change mitigation objectives. Indeed, different biomass resources have been proposed for the SESR process. Experimental works in the literature have studied bioethanol,[8−10] glycerol,[11−13] bio-oil from biomass pyrolysis,[14−17] or biogas[18,19] as feedstock. Biogas is a versatile raw material with a high potential to be utilized in reforming processes since it can be used as an alternative renewable source of CH_4.[20,21] Increasing interest in biogas also arises from reducing the dependence on fossil fuels and greenhouse gas emissions;[22] therefore, hydrogen production from biogas has great potential in a future-to-be CO_2 neutral or negative economy.[23] Biogas is produced from biomass, residues, or wastes by anaerobic digestion, being the gas generated in landfill sites also named biogas. Depending on its origin, it has a wide range of CH_4 (35−75 vol %) and CO_2 (25−55 vol %) contents, which are its major constituents, although it could contain other minority compounds such as H_2S, NH_3, siloxanes, and aromatics.[24] High CH_4 content biogas can directly generate heat or electricity, but low-grade biogas (low CH_4 content) is inappropriate for such purposes; hence, large quantities of poor-quality biogases are wasted by venting into the atmosphere.[25]

The main challenge of the SESR processes is the heat required for sorbent regeneration. In fact, the optimization of the energy demand in the process and the development and implementation of robust heat and energy recovery systems have been recently highlighted as key existing challenges for viable H_2 production by sorption enhanced processes.[26] As mentioned above, the SR reaction of methane is highly endothermic, but the WGS and the carbonation reactions are exothermic. Thus, the heat generated by the carbonation and WGS reactions balances the heat demand for reforming, so the reactor where the SESR step occurs is thermally neutral or slightly exothermic (eq 4). However, the subsequent sorbent regeneration step by the calcination reaction is endothermic, so overall the process requires energy.

Theoretically, the SESR of biogas is more exothermic than the SESR of pure methane since CO_2 in the biogas is also removed from the gas phase by the carbonation reaction[18] and provides additional heat into the system. It could be an advantage regarding the energy demand of the process. The CO_2 content in biogas can also have some drawbacks for the SESR process, such as a higher sorbent demand, a lower H_2 yield, or an increase in the equipment size, but these issues are out of the scope of the present work and need to be analyzed in a future techno-economic study of the process. However, to study the effect of the addition of CO_2 in the feeding, an energy analysis by simulation of the SESR process of biogas is needed to understand the thermodynamic limitations of the system under possible process configurations and optimize the energy efficiency.

Some works have performed simulation studies of the SESR process showing its advantages over SR regarding exergy efficiency. Tian et al.[27] reported the exergetic evaluation of the hydrogen production comparing SESR and conventional SR of acetic acid, finding a better performance (98.67% H_2 purity at 450−600 °C) and a 5% higher exergy efficiency in the SESR system. Tzanetis et al.[28] also compared the SESR with conventional SR of methane, finding an increase of 17.3% in the H_2 purity and 3.2% in the exergy efficiency. However, to optimize the energy efficiency of SESR processes, some works have proposed the coupling of SESMR with chemical looping combustion (CLC) for hydrogen production from methane. Alam et al.[29] proposed an efficient process for high purity hydrogen production by integrating SESMR with CLC obtaining an energy efficiency of 70.3%. Yan et al.[30] reported energy efficiency values of 72% for a process integrating SESMR with CLC and 74% for SESMR with oxy-fuel combustion integration. However, the CO_2 capture was higher when coupling CLC or oxy-fuel combustion to the SESMR process using air in the calcination reactor. Other authors have compared SESR and sorption enhanced chemical looping reforming (SECLR) of methane for hydrogen production, reporting higher H_2 yield and purity values in the case of SESMR, but lower energy requirements and higher CO_2 capture in the case of SECLR.[31,32] On the other hand, an autothermal sorbent regeneration process using combined combustion, methane reforming, and a hydrogen-selective membrane in the regenerator has been simulated by Ebneyamini et al.[33] Despite the possible improvements in energy efficiency by SESR integration with CLC or selective membranes use, those processes require additional devices, such as membrane reactors or separate reactors for reoxidation of the oxygen carrier. These unavoidably increase the equipment costs and provide less efficient heat integration.[34] A techno-economic evaluation of the overall processes should therefore be considered. In the case of the SESR of biogas for high purity hydrogen production, little work has been done on the topic, and studies addressing thermodynamic analysis and process simulations are very limited in the literature. Barelli et al.[35,36] performed a thermodynamic study of the hydrogen production with CO_2 capture of different gas mixtures, such as

https://doi.org/10.1021/acssuschemeng.2c07316
ACS Sustainable Chem. Eng. 2023, 11, 4759−4775

syngas and biogas, reaching adiabatic reforming for methane contents in the feed gas of 55%−65% and obtaining hydrogen purity higher than 99% and energy efficiency of 72%. However, a simulation of the SESR process using biogas is still needed to understand the energy utilization under different process configurations, taking advantage of the additional heat that CO_2 in the biogas may provide to the system.

For this purpose, a thermodynamic approach to process modeling is needed to demonstrate the thermodynamic feasibility of the process and provide the optimal process operating conditions and configurations that maximize energy efficiency when using biogas as feedstock. These results will be crucial for future work on the dynamic analysis of the process under the optimal SESR configuration that enables the scaling-up of the technology. The present work hence proposes different process layouts for renewable hydrogen production from biogas SESR, targeting the recovery of the heat released in the reformer while maximizing CO_2 capture. The process has been designed to be energy self-sufficient, hence avoiding the use of external utilities. This work aims to investigate the thermodynamic limitations of the different case studies on a wide range of process conditions, being the kinetic limitations and detailed reactor/auxiliaries design out of the simulation scope. The SESR process was simulated in Aspen Plus, including sorbent regeneration for a cyclic operation and using a heat exchanger network (HEN) to recover the waste heat from the process. With the further ambition to reduce the CO_2 emissions, we have also addressed oxy-combustion capture. Thus, five possible cases studies using three different process configurations have been evaluated to address the potential energy efficiency of the SESR process for a wide range of biogas compositions while maximizing the CO_2 capture. A detailed parametric analysis on biogas compositions, reforming temperature, pressure, and steam to methane (S/CH_4) ratio effect on the process performance is included. Different key performance indicators (KPIs) are discussed for all cases, such as H_2 purity, H_2 yield, CH_4 conversion, cold gas efficiency (CGE), net efficiency (NE), fuel consumption for the sorbent regeneration, and CO_2 capture efficiency.

MODEL DEVELOPMENT AND PROCESS CONFIGURATIONS

Herein, an autothermal SESR process of biogas that includes a first stage of steam reforming coupled with in situ CO_2 capture and a second stage of sorbent regeneration is built in Aspen Plus V11 software (AspenTech). The equilibrium model developed assumes steady-state conditions. The model includes a HEN to recover all the possible heat from the process streams. Three different SESR flowsheet base configurations (Figure 1) are comprehensively analyzed in this section alongside the model design and the different case studies (i.e., using different atmospheres for sorbent recovery). The detailed Aspen Plus flowsheets for the five case studies are shown in the Supporting Information (SI).

Model Development. The thermodynamic modeling assumptions used as the base design of the process to develop the different flowsheets are collected in Table 1. Biogas is simulated as a mixture of CH_4 and CO_2, while the solid sorbent is simulated as pure CaO.

Using the baseline conditions shown in Table 1, the range of the different variables studied is shown in Table 2.

The base flowsheet of the process mainly consists of two reactors: a reformer (SESR) and a calciner (REG). In the

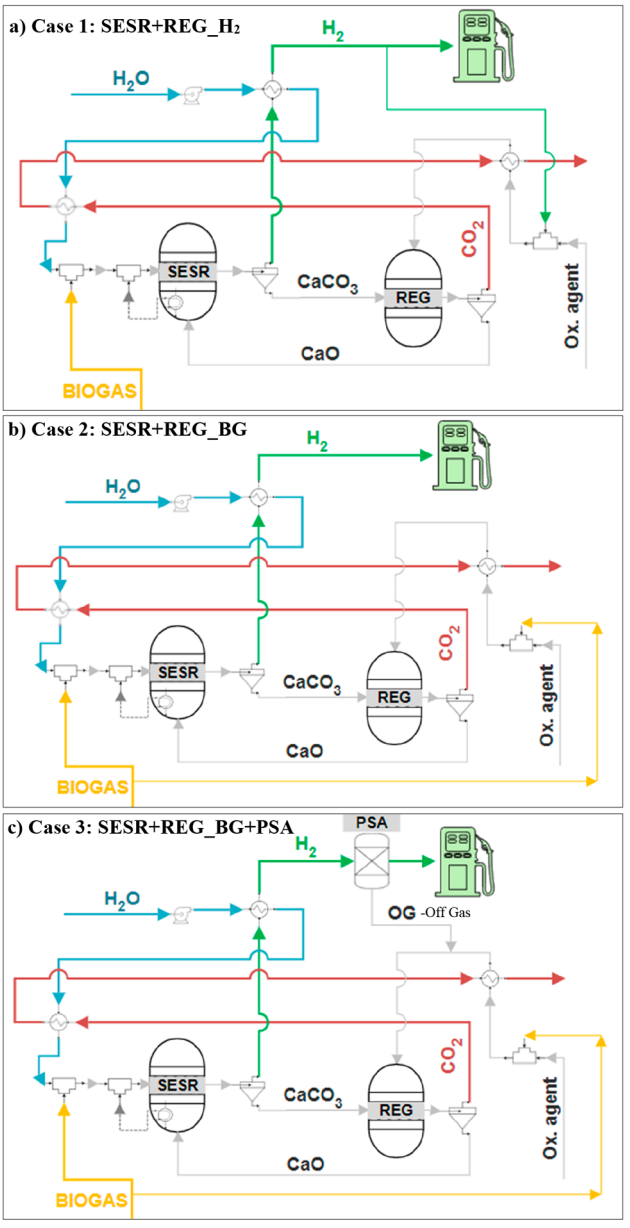

Figure 1. Simplified flow diagrams of the three base configurations proposed for the biogas SESR process. In Case 1 (SESR+REG_H_2), a fraction of the produced H_2 is used as fuel for the sorbent regeneration (a). In Case 2 (SESR+REG_BG), biogas is utilized as fuel for the sorbent regeneration (b). Finally, in Case 3 (SESR +REG_BG+PSA), biogas is used as fuel for the sorbent regeneration, and a PSA unit is included (c).

SESR reactor, biogas is the feedstock, and H_2 is rich in the product due to coexistence of the SR (eq 2), WGS (eq 3), and carbonation for CO_2 capture (eq 1) reactions. Due to the CO_2 removal, the equilibrium of SR and WGS reactions shifts toward a higher H_2 production according to Le Chatelier's principle. Furthermore, owing to the extra content of CO_2 in the biogas, the carbonation reaction turns pivotal in the overall duty of the SESR unit, which could be highly exothermic when biogas is used as feedstock.[37] The model developed in this work includes the extra heat recovery from the SESR unit to achieve an autothermal operation, assuming in the flowsheet design a 10% of heat loss during the heat transfer.[30] This value agrees with the thermal efficiency of reverse flow reactors,

https://doi.org/10.1021/acssuschemeng.2c07316
ACS Sustainable Chem. Eng. 2023, 11, 4759−4775

Table 1. Design Assumption Made to Develop the Base Case Flowsheet in Aspen Plus

Parameters	Value	Unit
Biogas feed	0.76 (13.33)	kg/s (MW[a])
Biogas composition (CH_4/CO_2)	60/40	vol %
Water feed inlet temperature	25	°C
Water feed inlet pressure	1	bar
Molar Ca/C ratio	1.5	–
Reformer pressure	10	bar
Reformer temperature	600	°C
Reformer molar steam/CH_4	5.5	–
Reformer heat loss	10	%
Calciner temperature	850	°C
Calciner pressure	1	bar
Excess oxygen[b]	5	%
Air/oxygen inlet temperature	25	°C
Air/oxygen pressure	1	bar
Fuel feed inlet temperature[c]	25	°C
Fuel feed pressure	1	bar
Calcination conversion	100	%
Heat exchanger pinch	20	°C
Isentropic efficiency of compressors and water pump efficiency	83	%
Mechanical efficiency of compressors and pump driver efficiency	98	%

[a]Based on LHV of CH_4 (800 MJ/kmol) and H_2 (242 MJ/kmol). [b]This refers to the excess oxygen (vol %) used in the REG reactor for the combustion of the fuel for sorbent regeneration. [c]Unless H_2 is used as fuel, in which case it enters the REG reactor at the reforming temperature.

Table 2. Range in Which the Different Process Variables Are Analyzed

Parameters	Range	Unit
Biogas composition (CH_4/CO_2)	50/50–80/20	vol %
Reformer temperature	500–675	°C
Reformer pressure	1.5–25	bar
Reformer molar steam/CH_4	3–6.5	–

which is a reactor type suggested to be sustainable for exothermic reactions.[38] From a practical point of view, to recover the heat released from the SESR reactor, a fluidized bed heat exchanger, consisting of a fluidized bed with heat exchanger tubes immersed in it, could be used.[5,39] Likewise, heat pipes have been suggested for indirect heating of the calciner in the chemical looping technology[40−42] and recently also for SESMR.[30]

On the other hand, the spent sorbent, forming $CaCO_3$, is separated from the H_2-rich gas stream and sent to the REG reactor, where the sorbent is regenerated to CaO to ensure process operation in a cyclic fashion. The spent sorbent is calcined, which is an endothermic reaction (reverse of eq 1) favored at high temperatures and low pressures (i.e., >800 °C and ∼1 bar).[43] Therefore, the calciner requires a high amount of heat to regenerate the sorbent. The desired temperature for the decomposition of $CaCO_3$ to CaO can be achieved by supplying heat by either burning a fuel in the calciner or indirect heating.[44,45] As shown in Figure 1, this work focuses on the direct combustion of renewable fuel to cover the duty required of the REG reactor using two fuel options: hydrogen and biogas. Moreover, two combustion atmospheres are under study: air and oxy-fuel combustion. In the case of using biogas, it matches the composition of the biogas feeding the SESR reactor for each particular simulation. The direct combustion of additional fuel in the calcination reactor seems to be the most practical option for providing the necessary heat.[15] The extra fuel feeding REG corresponds to the minimum needed to fulfill the duty of this unit. Hence, combustion proceeds without incomplete oxidation products (i.e., CO, H_2, or elemental C) leaving the REG reactor.[23] This is controlled by using different design specifications. The regeneration temperature used is 850 °C unless otherwise specified, ensuring that the regeneration of CaO is performed at 1 bar since low pressures are favorable for the calcination reaction (reverse of eq 1).

It is well-known that CaO-based sorbents suffer from conversion decay over cycles due to sintering.[46,47] Similarly to calcium looping systems, sorbent deactivation in SESR is handled by more often replacing the sorbent and controlling the particle size of the sorbent material. However, this is a practical issue that does not apply to evaluate the thermodynamic feasibility, which is the purpose of the present work. In the simulation, an average carbonation conversion of 50% was assumed for the CaO-based sorbent, according to the results of cyclic SESR experiments shown in the literature.[48,49] It can be maintained by ensuring an efficient makeup flow of the fresh/spent sorbent particles under the experimental operation of the process. Besides, this value has been used to estimate the molar Ca/C ratio in the reformer during the simulation following the Ca/C ratio in the reformer in a recent simulation study on blue hydrogen production by SESMR.[30] Therefore, a molar Ca/C ratio of 1.5 is selected, where C refers to the carbon contained in both CH_4 and CO_2 in the biogas fed to the SESR unit. All the calcium accounted for the Ca/C molar ratio comes from the CaO, initially added in excess, circulating between SESR and REG.

The reformer (SESR) and calciner (REG) were simulated using RGibbs blocks, as suggested in other modeling studies in the literature.[23,30] The Aspen Plus flowsheets are shown in Figures S1−S6 of the Supporting Information. In this work, it is assumed that all the reactions in both reactors, SESR and REG, reach chemical equilibrium, and the entire process operates under a steady state. The chemical equilibrium of the reforming and regeneration reactors is calculated by minimization of the Gibbs free energy. The species considered were H_2, CH_4, CO, CO_2, H_2O, O_2, N_2, CaO, $Ca(OH)_2$, and $CaCO_3$. C_2H_4, C_2H_6, and C (solid carbon graphite to account for the possible formation of coke) were also in the product pool, but their concentrations at equilibrium were negligible under the studied conditions. Physicochemical properties of all the components included in the process are determined using Peng−Robinson's equation of state.

Furthermore, a HEN was designed to recover the maximum heat from the process streams with a minimum number of heat exchangers (Figures S1−S5 of Supporting Information). It aims not only to preheat the reactants but also to produce the steam needed for the reforming avoiding the energy penalty of its production. In the HEN, water is preheated in HE1 using the maximum heat extracted from the hydrogen stream from the SESR reactor while avoiding condensation by specifying 5 °C of superheat at the outlet of the hot stream. Any heat produced during steam condensation is considered non-recoverable heat.[23] Then, the evaporation continues in HE2 using the CO_2 stream from the REG reactor; another heat exchanger, H1 (which uses the heat released from the SESR

https://doi.org/10.1021/acssuschemeng.2c07316
ACS Sustainable Chem. Eng. 2023, 11, 4759−4775

Table 3. Case Studies Evaluated for Energy Integration of SESR Process of Biogas

Process configuration	Sorbent regeneration atmosphere	Sorbent regeneration fuel	H_2 purification
Case 1: SESR+REG_H2	Air	H_2	–
Case 2: SESR+REG_BG	Air	Biogas	–
	Oxy-fuel	Biogas	–
Case 3: SESR+REG_BG+PSA	Air	Biogas + PSA off-gas	PSA
	Oxy-fuel	Biogas + PSA off-gas	PSA

reactor), is used to complete the steam production when needed and to preheat the SESR reactants to reach the reaction temperature. A design specification calculates the minimum amount of energy required in HE2 from the CO_2-rich stream to force the duty of H1 to equal the amount of energy available from SESR (assuming 10% of heat losses). By doing this, the energy balance of the process is matched. Finally, the energy that remains in the CO_2 stream is used to preheat the inlet streams of the REG reactor, using a heat exchanger pinch of 20 °C to maximize the heat recovery from this stream. The exhausted hydrogen-rich gas is cooled down in a cooler (C1) to 25 °C to condensate and separate most of the water in a separation unit (SEP1). The dry H_2 stream is then ready for the downstream processing (i.e., purification, compression, etc.) according to the application.

Process Configurations. Three process configurations were designed (simplified diagrams shown in Figure 1) and five case studies compared (Aspen Plus flowsheets shown in Figures S1−S5 of Supporting Information). The description of each case study is summarized in Table 3. In the first configuration (Figure 1a), the use of a fraction of the produced H_2 as a renewable fuel to supply energy for sorbent regeneration through calcination is studied (SESR +REG_H_2), whereas in the second process configuration (Figure 1b) biogas is used for this purpose (SESR+REG_BG). In Case 1, SESR+REG_H_2, the recycled H_2 contains mainly hydrogen, unreacted CH_4, and trace quantities of CO and CO_2. The amount of hydrogen recycled to the REG reactor is calculated with a design specification to fulfill the energy requirement of the unit and to avoid incomplete oxidation products, as previously explained. In Case 2, SESR+REG_BG, the amounts of fuel (i.e., biogas) and oxidant agent needed are calculated similarly using design specifications. Moreover, in the third configuration, represented by Case 3 (Figure 1c), the dry hydrogen product (H2RICH) is further purified using a pressure swing adsorption (PSA) unit (SESR+REG_BG+PSA) to increase the hydrogen product purity up to levels that allow its use in applications as fuel cells. A compressor is placed before the PSA unit to maintain the inlet stream at a pressure higher than 25 bar, which is the typical operating pressure for PSA. In this work we have set a fixed backup pressure of 30 bar. The off-gas from the PSA unit (PSA-OG) contains mainly H_2 and CH_4 and trace quantities of CO and CO_2, and it is sent to the calciner to reduce the amount of additional biogas required as fuel. The separation efficiency of the PSA unit is set at 95%.[30] In practice, the recovery rate and purity of H_2 after PSA purification will depend on a range of factors (i.e., gas volume handled, adsorption material, temperature and pressure differences, etc.) and should take into account the presence of trace gases (i.e., CO) depending on the final H_2 application, but detailed modeling of the PSA unit is out of the scope of this work.

In all cases, a compressor with 83% isentropic efficiency and 98% mechanical efficiency[30] is placed to match the operating pressure of the reactor (which varies in the different simulations). Similarly, a water pump with the same efficiencies matches the pressure of the water stream used to produce the steam. Furthermore, the flow of oxidant agent used in the REG unit is controlled to meet a 5% excess of oxygen.[30] Thus, in the calciner, not only direct combustion using air is analyzed (Figures S1, S2, and S4 of Supporting Information), but also oxy-fuel combustion (30% O_2 and 70% CO_2 mole fraction gas supplied to REG reactor) is studied (Figures S3 and S5 of Supporting Information) to evaluate the reduction in CO_2 emissions. This resulted in a total of five scenarios: Cases 2 and 3 with direct oxy-fuel and air combustion and Case 1 with direct air combustion in the calciner. Due to the challenges associated with hydrogen in oxy-combustion (high temperatures and overheating, flame instability, flame blowout) derived from its broader flammability range, much higher adiabatic flame temperature, and higher flame propagation rate, the oxy-fuel scenarios have been restricted to biogas used as fuel.

Data Evaluation. Thermodynamic performance of the process is evaluated in terms of H_2 purity, H_2 yield, CH_4 conversion, cold gas efficiency (CGE), net efficiency (NE), fuel consumption in REG unit, and CO_2 capture efficiency. These parameters have been selected as the key process performance indicators (KPIs) of the biogas SESR process to compare all the case studies in this research work. H_2 purity is calculated by eq 5, where y_i is the molar content (N_2 free and on dry basis) of each species i in the outlet gas. H_2 yield represents the percentage of H_2 produced in the plant to the maximum H_2 production according to the SESR reaction stoichiometry, and it is calculated by eq 6, where $F_{H2,out}$ is the molar flow rate of hydrogen produced, and $F_{CH4,in}$ is the molar flow rate of methane fed in. CH_4 conversion is calculated by eq 7, where $F_{CH4,in}$ and $F_{CH4,out}$ are the molar flow rates of CH_4 in the inlet (BIOGAS) or outlet (H_2) streams, respectively.

$$H_2\ \text{purity (vol \%)} = 100\cdot(y_{H2}/\Sigma_i y_i) \tag{5}$$

$$H_2\ \text{yield (\%)} = 100\cdot(F_{H2,out}/(4\cdot F_{CH4,in})) \tag{6}$$

$$CH_4\ \text{conversion (\%)} = 100\cdot((F_{CH4,in} - F_{CH4,out})/F_{CH4,in}) \tag{7}$$

CH_4, CO_2, and CO concentrations are also calculated by eq 8.

$$CH_4/CO_2/CO\text{(vol \%)} = 100\cdot(y_{CH4/CO2/CO}/\Sigma_i y_i) \tag{8}$$

On the other hand, the CGE is calculated as the ratio between the chemical energy of the produced H_2 stream to the sum of the feed thermal input (chemical energy of the CH_4 feed consumed in the SESR reactor and the additional CH_4 required to meet the heat requirements of the REG reactor). CGE is calculated by eq 9, where $F_{CH_4,\ additional}$ is the molar flow rate of methane contained in the additional biogas fed in the calciner to meet the duty requirement of the REG unit. The

https://doi.org/10.1021/acssuschemeng.2c07316
ACS Sustainable Chem. Eng. 2023, 11, 4759−4775

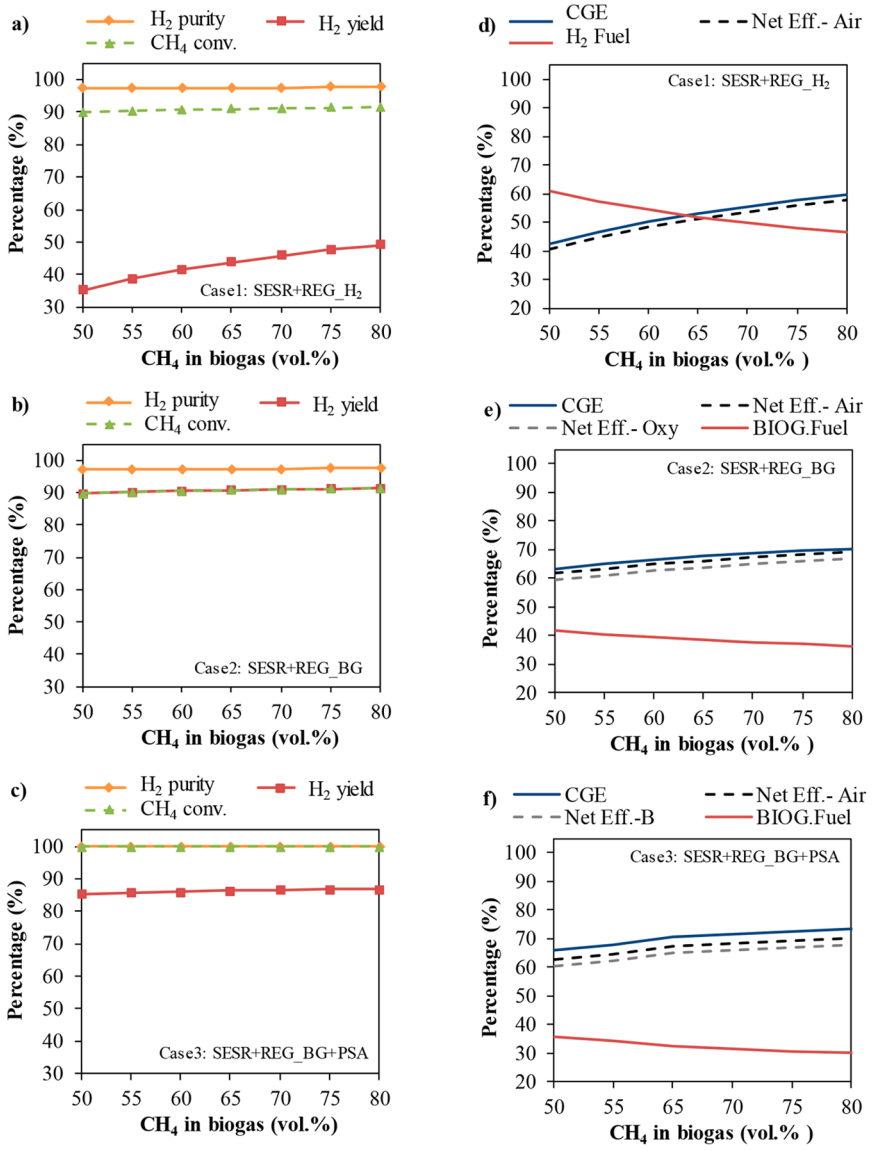

Figure 2. Effect of biogas composition on H_2 purity, H_2 yield, and CH_4 conversion (a–c) and on cold gas efficiency (CGE), net efficiency (NE, using both air, Net Eff. A, and oxy-combustion, Net Eff-B, in REG), and fuel consumption for sorbent regeneration (d–f) for the different process configurations studied: (a, d) use of a fraction of the produced hydrogen as fuel for sorbent regeneration (SESR+REG_H_2), (b, e) use of biogas as fuel for sorbent regeneration (SESR+REG_BG), and (c, f) addition of a PSA unit and use of biogas and off-gas (PSA-OG) for sorbent regeneration (SESR+REG_BG+PSA). SESR conditions: S/CH_4 = 5.5, T = 600 °C, P = 10 bar, and 50% sorbent excess.

LHV_{H_2} and LHV_{CH_4} are the lower heating value of hydrogen (242 MJ/kmol) and methane (800 MJ/kmol), respectively. NE is calculated by eq 10, where the electric utility requirement of the auxiliaries (P_e) is added to the CGE equation where a thermal to electric conversion efficiency (η_{elect}) of 50% is applied, and for the oxy-combustion scenarios, 160 kWh/t of oxygen is assumed as the auxiliary power consumption of the air separation unit (ASU).[30] The fuel consumption in Case 1 (SESR+REG_H_2) is calculated by eq 11, whereas in Case 2 (SESR+REG_BG) and Case 3 (SESR +REG_BG+PSA) it is calculated by eq 12.

$$\mathrm{CGE}\ (\%) = \left(\frac{F_{H_2,\mathrm{out}}\cdot \mathrm{LHV}_{H_2}}{(F_{CH_4,\mathrm{in}} + F_{CH_4,\mathrm{additional}})\cdot \mathrm{LHV}_{CH_4}}\right)\cdot 100 \quad (9)$$

$$\mathrm{NE}\ (\%) = \left(\frac{\mathrm{F}_{H_2,\mathrm{out}}\cdot \mathrm{LHV}_{H_2}}{(F_{CH_4,\mathrm{in}} + \mathrm{F}_{CH_4,\mathrm{additional}})\cdot \mathrm{LHV}_{CH_4} + \frac{P_e}{\eta_{\mathrm{elect}}}}\right)\cdot 100 \quad (10)$$

$$\mathrm{Fuel}_{H_2,\mathrm{recycled}}(\%) = \left(\frac{F_{H_2,\mathrm{recycled\ to\ REG}}}{F_{H_2,\mathrm{recycled\ to\ REG}} + F_{H_2,\mathrm{out}}}\right)\cdot 100 \quad (11)$$

$$\mathrm{Fuel}_{\mathrm{Biogas}}(\%) = \left(\frac{F_{\mathrm{Biogas\ fed\ to\ SESR}}}{F_{\mathrm{Biogas\ fed\ to\ SESR}} + F_{\mathrm{Biogas\ fed\ to\ REG}}}\right)\cdot 100 \quad (12)$$

Finally, the CO_2 capture efficiency is calculated by eq 13, where $F_{CO2,captured}$ is the molar flow of CO_2 in the outlet CO_2 stream.

https://doi.org/10.1021/acssuschemeng.2c07316
ACS Sustainable Chem. Eng. 2023, 11, 4759–4775

$$\text{CO}_2 \text{ capture efficiency (\%)} = \left(\frac{F_{\text{CO}_2,\text{captured}}}{F_{\text{CH}_4,\text{in}} + F_{\text{CH}_4,\text{additional}} + F_{\text{CO}_2,\text{in}} + F_{\text{CO}_2,\text{additional}}} \right) \cdot 100 \quad (13)$$

RESULTS AND DISCUSSION

A sensitivity analysis has been performed for the three process configurations studied: (1) SESR with a H_2-fired calciner (SESR+REG_H_2), (2) SESR realized using biogas for the sorbent regeneration (SESR+REG_BG), and (3) SESR realized using biogas for the sorbent regeneration and with a pressure swing adsorption (PSA) unit (SESR+REG_BG +PSA); the cases were analyzed under air (all) and oxy-fuel combustion (when using biogas as fuel in the calciner), respectively, resulting in five case studies.

Effect of Biogas Compositions. The effects of the biogas compositions on H_2 purity, CH_4 conversion, and H_2 yield are shown in Figure 2a–c. The range of compositions studied increases to 80% of CH_4 since a high concentration of methane could be obtained after a slight biogas purification step, so this case is included for comparison purposes. In Cases 1 and 2 (Figure 2a and b, respectively), H_2 purity slightly increases from 97.1% to 97.6% for the high methane concentrations in the feed stream from 50 to 80 vol %. However, H_2 purity achieves nearly 100 vol % in Case 3 with the PSA purification unit (Figure 2c). This indicates biogas compositions do not significantly change the H_2 purity obtained after SESR, in good agreement with the experimental results reported in our previous proof of concept.[18] Furthermore, the results show that the recovery of the extra heat produced in the SESR step with the proposed designs allows for achieving autothermal operation of the reformer, independently of the biogas composition.

For Cases 1 and 2, CH_4 conversion increases slightly from 89.8% to 91.5% with CH_4 content in biogas, similarly to the H_2 purity, so the same results are obtained when a fraction of the produced H_2 is used as fuel for sorbent regeneration (Figure 2a) than when biogas is used as fuel in the REG reactor (Figure 2b). On the other hand, the addition of the PSA unit and the subsequent recycling of the off-gas (PSA-OG) to the REG reactor, i.e., Case 3, increase the CH_4 conversion to 100% since the unreacted CH_4 from the SESR unit is recirculated with PSA-OG to the REG reactor where it burns off (Figure 2c).

Finally, H_2 yield is very low in Case 1 (Figure 2a) due to the use of a fraction of the produced hydrogen as a renewable fuel to fulfill the energy duty of the sorbent regeneration stage. It increases from 35.2% to 49.1% in the range of the biogas compositions analyzed, i.e., 50 to 80 vol % of CH_4 (balance CO_2). The highest H_2 yield is obtained in Case 2, biogas used as fuel in REG (Figure 2b) without the PSA-OG recycle: 89.7% to 91.4% for 50 to 80 vol % of CH_4 in biogas. When recycling the PSA-OG in Case 3 (Figure 2c), the H_2 yield lowers since the off-gas contains not only the unreacted CH_4 from SESR but also a small fraction of H_2 (we assumed a PSA efficiency of 95%), and it increases from 85.3% to 86.9% for 50 to 80 vol % of CH_4 in biogas. Therefore, the composition of biogas has little effect on the H_2 yield, in agreement with the slight increase in CH_4 conversion.

The efficiencies, CGE and NE, for the different configurations and the percentage of fuel consumed for sorbent regeneration are shown in Figure 2d–f as a function of the biogas composition (50 to 80 vol % of CH_4, balance CO_2). Process configurations have been evaluated using air (all) and oxy-combustion (when using biogas as fuel) atmospheres. The only differences detected in the results between both combustion atmospheres are in the net efficiency of the overall process, due to the additional auxiliary power consumption of the air separation unit (ASU) in the case of oxy-fuel combustion. This small difference in NE is explained because the direct heating approach relies on a sorbent regeneration by decreasing the CO_2 partial pressure during the direct combustion of the fuel in the calciner at a temperature <900 °C.

In Case 1, where produced H_2 is used as fuel in REG, CGE increases a total of 16.8%, from 42.5% to 59.4%, with CH_4 content in the biogas (Figure 2d). In Case 2 (Figure 2e), where biogas is directly combusted in the calciner, CGE increases from 63.2% to 70.3% as CH_4 content in the biogas increases, meaning a total increase of 7.1%. Finally, for Case 3 (Figure 2f), when a PSA unit is utilized, CGE increases from 66.1% to 73.5%, which means a total increase of 7.4%. The increasing tendency in the CGE value with CH_4 content in the biogas agrees with the results reported by Kong et al.[23] for biogas conversion to H_2 using chemical looping (CL) technology. CGE values are dependent on the amount of fuel used in REG, so they indicate that the use of biogas as renewable fuel for sorbent regeneration (Case 2) renders better results than the use of produced H_2 (Case 1). On the other hand, Case 3 has the highest CGE value due to the positive effect of the further H_2 purification with the PSA unit and the subsequent recycling of the off-gas to the REG reactor. It is explained because the recycle allows a notable decrease in the fuel consumption (Figure 2f) compared to other configurations. NE values follow the same increasing tendency with the CH_4 content in the biogas as those for CGE. When combustion is carried out under an air atmosphere, in Cases 1 and 2, NE is 1.6% points below CGE due to the electric utility requirement of the auxiliaries considered. However, NE is 3.3% lower than CGE for Case 3 due to the additional compressor needed to match the pressure required by the PSA unit. When combustion in REG is carried out under oxy-combustion conditions, NE is 2.3%–2.5% lower than that obtained for the air atmosphere due to the energy penalty of the ASU.

On the other hand, Table 4 shows the effect of the biogas composition on the heat recovery from the SESR reactor. The amount of energy recovered from SESR varies from 3.9 MW (50 vol % CH_4 in biogas) to 2.5 MW (80 vol % CH_4 in biogas) for the same amount of biogas treated (100 kmol/h). This

Table 4. Effect of Biogas Composition on Heat Recovered from SESR (Heat Losses Considered)[a]

Biogas composition	Heat recovered from SESR (MW)
50% CH_4–50% CO_2	3.9
55% CH_4–45% CO_2	3.7
60% CH_4–40% CO_2	3.4
65% CH_4–35% CO_2	3.2
70% CH_4–30% CO_2	3.0
75% CH_4–25% CO_2	2.8
80% CH_4–20% CO_2	2.5

[a]SESR conditions: S/CH_4 = 5.5, T = 600 °C, P = 10 bar, and 50% sorbent excess.

https://doi.org/10.1021/acssuschemeng.2c07316
ACS Sustainable Chem. Eng. 2023, 11, 4759–4775

Table 5. Excess of Heat Not Used That Is Remaining in CO_2 Stream as a Function of Biogas Composition[a]

	Excess heat not used in CO_2 stream (MW)		
Biogas composition	Case 1: SESR+REG_H_2	Case 2: SESR+REG_BG	Case 3: SESR+REG_BG + PSA
50% CH_4–50% CO_2	1.8	1.7	1.7
55% CH_4–45% CO_2	1.5	1.4	1.5
60% CH_4–40% CO_2	1.3	1.2	1.2
65% CH_4–35% CO_2	1.0	1.0	1.0
70% CH_4–30% CO_2	0.7	0.8	0.8
75% CH_4–25% CO_2	0.4	0.6	0.6
80% CH_4–20% CO_2	0.1	0.4	0.4

[a]SESR conditions: S/CH_4 = 5.5, T = 600 °C, P = 10 bar, and 50% sorbent excess.

results from a balance between the carbonation and reforming reactions: when CO_2 content in biogas is higher, carbonation occurs to a greater extent, and more heat is released in the SESR reactor. These results explain the higher excess heat in the final CO_2 stream for biogas with lower concentrations of CH_4 that is shown in Table 5; more heat is recovered from the SESR reactor, and hence more heat remains in the CO_2 stream. The excess heat in the outlet CO_2 stream has been calculated as the maximum recoverable heat while ensuring the avoidance of condensation by specifying 5 °C of superheat at the outlet of the hot stream; i.e., any heat produced during steam condensation is considered nonrecoverable heat.[23] As mentioned above, more heat is available in this stream for the lower CH_4 content in biogas, highlighting the potential interest of using low grade biogas compared to natural gas due to heat recovery from this hot stream.

Therefore, if a waste heat recovery system was employed to recover the heat available in the final CO_2 stream, the overall CGE values of the process could increase for all biogas compositions to similar values to those reached with higher methane concentrations. It has been demonstrated as an example for Case 3 with air regeneration and shown in Figure 3, where the surplus heat in the outlet CO_2 stream has been employed in the regeneration reactants preheating.

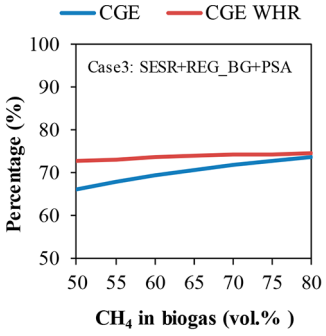

Figure 3. Comparison of the CGE with (red line) and without (blue line) waste heat recovery (WHR) from the CO_2 stream for the Case 3 (SESR+REG_BG+PSA).

Effect of SESR Reactor Temperature. The effects of the reforming temperature on H_2 purity, CH_4 conversion and H_2 yield, CGE, NE, and percentage of fuel consumed by sorbent regeneration are shown in Figure 4a–f. The results for H_2 purity, CH_4 conversion, H_2 yield, CGE, and fuel consumption remain unchanged when using air or oxy-combustion atmospheres for the sorbent regeneration, and only NE is affected. In Cases 1 and 2 (Figure 4a and b), where H_2 and biogas are used as fuels for regeneration, respectively, without a PSA unit, H_2 purity increases from 91.0% to 98.3% as the SESR temperature rises from 500 to 625 °C due to the endothermic nature of the SR reaction (eq 2). When the temperature further increases from 625 up to 675 °C, H_2 purity slightly decreases (by ∼0.4%) since the enhancement effect of the in situ CO_2 capture is thermodynamically unfavorable at higher temperatures because the carbonation reaction is exothermic (eq 1).[16,50] In Case 3 (Figure 4c), where biogas is used as fuel for regeneration but adding a PSA step, H_2 purity achieves nearly 100 vol % for all SESR temperatures due to the PSA unit, which performs a further purification of the hydrogen rich stream.

CH_4 conversion in Cases 1 and 2 significantly increases from 71.8% to 94.5% as SESR temperature increases up to 625 °C, also due to the endothermic SR reaction; afterward, it only slightly increases with a further increase in temperature (by ∼0.4%). With the addition of the PSA unit and the use of the off-gas (PSA-OG) in REG (Case 3), the CH_4 conversion reaches a constant value of 100% for all SESR temperatures (Figure 4c) since PSA-OG contains the unreacted CH_4 from SESR, which then burns in the REG reactor.

On the other hand, the lowest H_2 yield is obtained in Case 1 due to the recycling of part of the H_2 produced in SESR as a fuel for the REG reactor. H_2 yield increases from 31.0% to 41.4% with the increase in the SESR temperature from 500 to 600 °C since higher temperatures favor the reforming reaction and, consequently, the methane conversion and hydrogen production. A faster increase is observed from 600 to 625 °C and then is kept around 50% above 625 °C. In Cases 2 and 3, H_2 yield also increases faster up to 625 °C, reaching values of 94.4% and 89.7%, respectively. As temperature further increases, a slight increase is seen up to 94.7% in Case 2 and 89.9% in Case 3. As explained above, when PSA-OG is combusted (Case 3), the H_2 yield is slightly lower, since the off-gas also contains a small fraction of H_2 because the PSA unit efficiency is 95%.

The higher increase detected in the H_2 yield value from 600 to 625 °C in Case 1 (Figure 4a) is related to the formation of solid $Ca(OH)_2$ below 600 °C since its formation is thermodynamically disfavored above 600 °C because the lime hydration reaction (eq 14) is exothermic.[51]

$$CaO_{(s)} + H_2O_{(l)} \leftrightarrow Ca(OH)_{2(s)} \quad \Delta H_r^0 = -67\,kJ\,mol^{-1} \tag{14}$$

As can be seen in Table 6, the excess sorbent not converted to $CaCO_3$ is in the form of $Ca(OH)_2$ below 600 °C but in the form of CaO above that temperature. It means that at lower SESR temperatures, $Ca(OH)_2$ is formed alongside $CaCO_3$ by carbonation, and both need to be regenerated and converted to CaO in the REG reactor. It requires more energy than that

https://doi.org/10.1021/acssuschemeng.2c07316
ACS Sustainable Chem. Eng. 2023, 11, 4759–4775

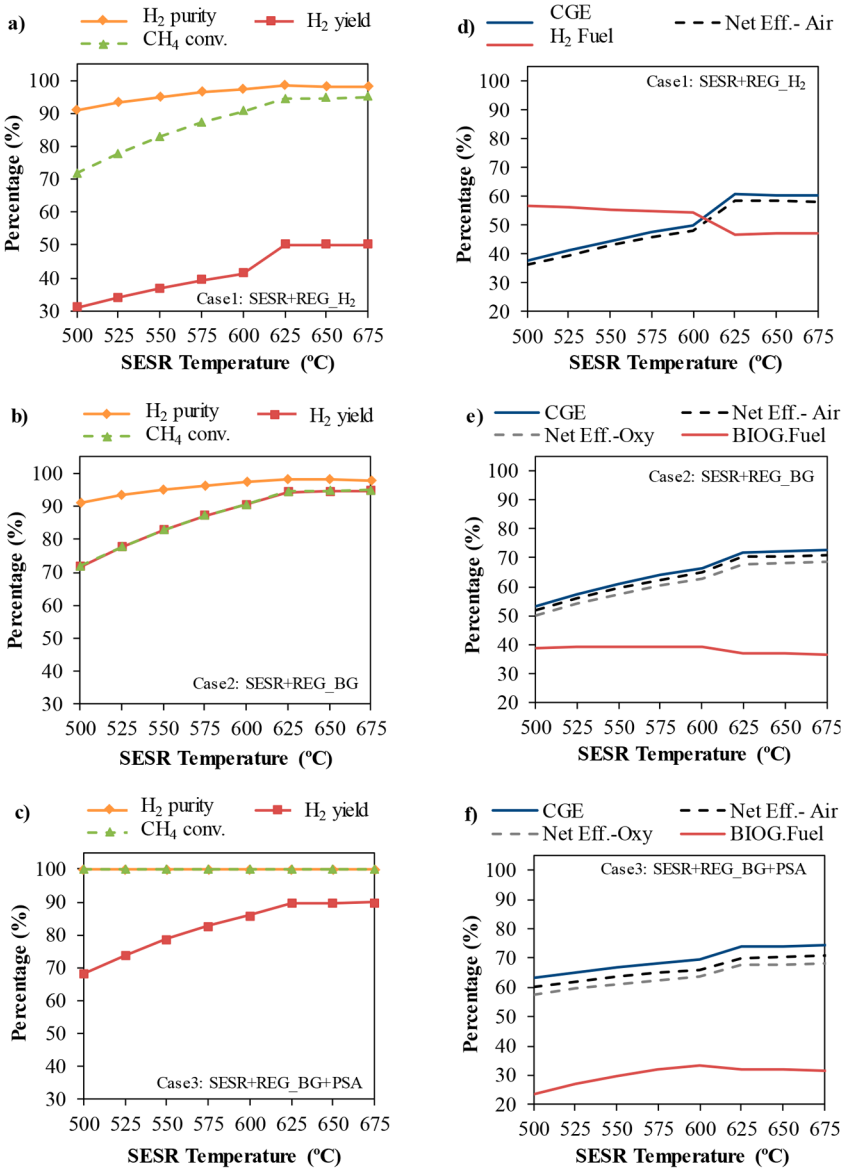

Figure 4. Effect of SESR temperature on H_2 purity, H_2 yield, and CH_4 conversion (a–c) and on cold gas efficiency (CGE), net efficiency (NE, using both air, Net Eff. A, and oxy-combustion, Net Eff-B, in REG), and fuel consumption for sorbent regeneration (d–f) for the different process configurations studied: (a, d) use of a fraction of the produced hydrogen as fuel for sorbent regeneration (SESR+REG_H_2), (b, e) use of biogas as fuel for sorbent regeneration (SESR+REG_BG), and (c, f) addition of a PSA unit and use of biogas and off-gas (PSA-OG) for sorbent regeneration (SESR+REG_BG+PSA). SESR conditions: S/CH_4 = 5.5, P = 10 bar, biogas = 60/40 vol % CH_4/CO_2, and 50% sorbent excess.

Table 6. Effect of SESR Temperature on Composition of Solids Circulating between SESR and REG[a]

	Solids composition at SESR outlet (%)		
SESR Temperature (°C)	$CaCO_3$	CaO	$Ca(OH)_2$
500	55.4	0.0	44.6
525	57.7	0.0	42.3
550	59.8	0.0	40.2
575	61.4	0.0	38.6
600	62.7	0.0	37.3
625	64.1	35.9	0.0
650	63.9	36.1	0.0
675	63.4	36.6	0.0

[a]SESR conditions: S/CH_4 = 5.5, P = 10 bar, biogas = 60/40 vol % CH_4/CO_2, and 50% sorbent excess.

needed when only $CaCO_3$ is formed and the unreacted sorbent remains as CaO. Therefore, more energy needs for REG means more H_2 needs to be recycled to cover the duty of the REG reactor at lower temperatures which, in turn, has a negative impact on H_2 yield.

Figure 4d–f shows that CGE and NE follow a similar tendency than H_2 yield. The effect of the $Ca(OH)_2$ formation at lower temperatures can be observed not only in Case 1 when recycling H_2 to REG but also in Cases 2 and 3 when using biogas as fuel in REG, affecting the efficiency values. However, the impacts for Cases 2 and 3 are lower because the heating value of biogas is higher than that of hydrogen, and the additional amount of biogas needed as fuel in those cases is lower, as observed in the fuel consumption in Figure 4d–f. On the other hand, low operating temperatures below 625 °C favor CO_2 removal according to the thermodynamics leading

https://doi.org/10.1021/acssuschemeng.2c07316
ACS Sustainable Chem. Eng. 2023, 11, 4759–4775

to a very low CO_2 content in the SESR outlet gas (Figure 5b). As reported by He et al.,[50] in the low temperature range, the

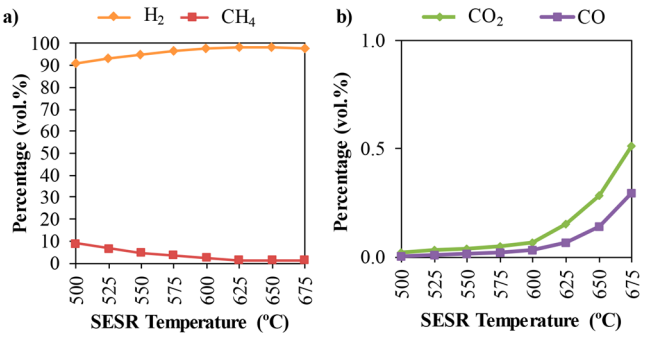

Figure 5. Effect of SESR temperature on H_2 and CH_4 concentrations (a) and CO_2 and CO concentrations (b) in the outlet gas from the SESR reactor in Case 1. SESR conditions: S/CH_4 = 5.5, P = 10 bar, biogas = 60/40 vol % CH_4/CO_2, and 50% sorbent excess.

endothermic reaction of methanation is favored by thermodynamics and might make an important contribution to CH_4 formation. Consequently, a higher content of CH_4 can be seen in the product gas of the SESR reactor at lower temperatures (Figure 5a).

Figure 4d–f shows that CGE increases noticeably as the SESR temperature increases up to 625 °C, as a consequence of the increase in methane conversion with temperature. At higher temperatures, only small variations (~0.5%) are observed. This is also in agreement with the decrease in the fuel consumption in REG for Cases 1 and 2 (Figure 4d and 4f) with the temperature increase due to a narrower temperature window between the reformer and calciner at a higher SESR temperature. However, in Case 3, with PSA-OG use in REG, the fuel consumption increases up to 600 °C (Figure 4f), and hence, the increase in the efficiency with temperature is less pronounced since it is affected by the change in the PSA-OG composition with the SESR temperature. As the temperature increases in the reformer, CH_4 conversion also increases, and less unreacted CH_4 is present in PSA-OG, which, in turn, enriches the off-gas in H_2. Conversely, at low SESR temperatures, the content of CH_4 in the PSA-OG is higher, the calorific value of the PSA-OG increases, and the process requires a lower amount of biogas as fuel for the sorbent regeneration. The overall positive tendency in the efficiency would result from the overall energy balance since, at higher SESR temperature, the solids circulating between SESR and REG are at closer temperature boosting the fulfilment of the REG energy requirement. Besides, it has been suggested in the literature that an increase in the carbonation reactor temperature could improve the efficiency of a plant involving carbonation–calcination cycles.[36] The CGE values at 625 °C are 60.7% and 72.0% in Cases 1 and 2, respectively, while it reaches 74.3% at 675 °C in Case 3. The addition of a PSA unit improves the efficiency due to the utilization of PSA-OG to provide more heat to the system. NE values when using air combustion in REG are lower than CGE values by ~1.80% in Cases 1 and 2 and 3.5% in Case 3. This is due to the additional compressor needed in Case 3 to match the pressure required by the PSA unit. When using oxy-combustion, the NE lowers (2.4% points) compared to the use of air due to the penalty associated with the oxygen production in the ASU.

The amount of energy recovered from the SESR reactor as a function of temperature decreases from 4.0 MW at 500 °C to 1.8 MW at 675 °C (see Table S1 of the Supporting Information). As the SESR temperature increases, so does the methane conversion, and the reforming reaction governs the heat balance. However, at lower temperatures, the carbonation reaction drives the heat balance since reforming is not favored; therefore, more heat released by carbonation is available in the SESR reactor. In addition, at lower temperatures, not only carbonation releases heat but also lime hydration that is slightly exothermic, and more heat is therefore available in SESR for recovery.

Effect of Pressure. Since high-pressure operation is a common practice in large-scale applications to reduce the reactor size and cost of H_2 production,[52] pressure is an important parameter to address. Furthermore, higher operating pressures could be of interest for SESR to apply a pressure swing to regenerate the CO_2 sorbent instead of increasing the temperature.[53] The effects of the reforming pressure on H_2 purity, CH_4 conversion, and H_2 yield for the different process configurations are shown in Figure 6a–c. In Cases 1 and 2 (Figure 6a and b), H_2 purity has a value of 99.0 vol % between 1.5 and 5 bar, decreasing until 91.4 vol % as pressure increases up to 25 bar. In Case 3 (Figure 6c), when a PSA unit is included, H_2 purity shows values of 100% along the pressure range since H_2 purity increases due to the additional capture step.

CH_4 conversion slightly decreases from 98.9% to 96.7% as SESR pressure increases from 1.5 to 5 bar in Cases 1 and 2. At higher pressures, CH_4 conversion decreases very sharply as pressure increases from 5 to 25 bar until a value of 73.0%. In agreement with the literature,[54] as pressure increases, the CH_4 conversion and H_2 purity decrease since SESR is thermodynamically favored at lower pressure due to the rise in the number of gas moles associated with the overall reaction which involves SMR and carbonation.[55] In addition, an increase in pressure promotes the formation of methane by the methanation reaction,[17,53] hence increasing the content of CH_4 in the gas coming out from SESR (Figure 7a). In Case 3 (Figure 6c), when a PSA unit is added, CH_4 conversion shows values of 100% for all pressures since the unconverted CH_4 from the SESR reactor is later used as fuel in the REG reactor through the PSA-OG combustion.

Regarding the H_2 yield, it also shows higher values at pressures of 1.5–5 bar, decreasing as pressure increases up to 25 bar. The highest H_2 yield values are obtained in Case 2 when only biogas is used as fuel in the REG reactor (Figure 6b), decreasing H_2 yield values from 98.7% at 1.5 bar to 96.7% at 5 bar (then decreasing until 73.0% at 25 bar). In Case 3 (Figure 6c), H_2 yield slightly lowers from 93.8% at 1.5 bar to 91.9% at 5 bar, decreasing down to 69.3% at 25 bar, due to the combustion of a small fraction of H_2 with the PSA-OG. Finally, in Case 1, H_2 yield is much lower, ranging from 51.3% at 1.5 bar to 50.4% at 5 bar (decreasing down to 33.9% at 25 bar) (Figure 6a) since a fraction of the produced hydrogen is used as fuel in the REG reactor. The decrease in this parameter above 5 bar is in accordance with the tendency observed for the CH_4 conversion and H_2 purity.

Higher electrical efficiency is expected in a solid oxide fuel cell (SOFC) when using H_2 produced at high pressure, as reported by Diglio et al.[52] Moreover, if the H_2 stream is going to be used in phosphoric acid fuel cells (PAFC) or low-temperature proton exchange membrane fuel cells (LT-

https://doi.org/10.1021/acssuschemeng.2c07316
ACS Sustainable Chem. Eng. 2023, 11, 4759–4775

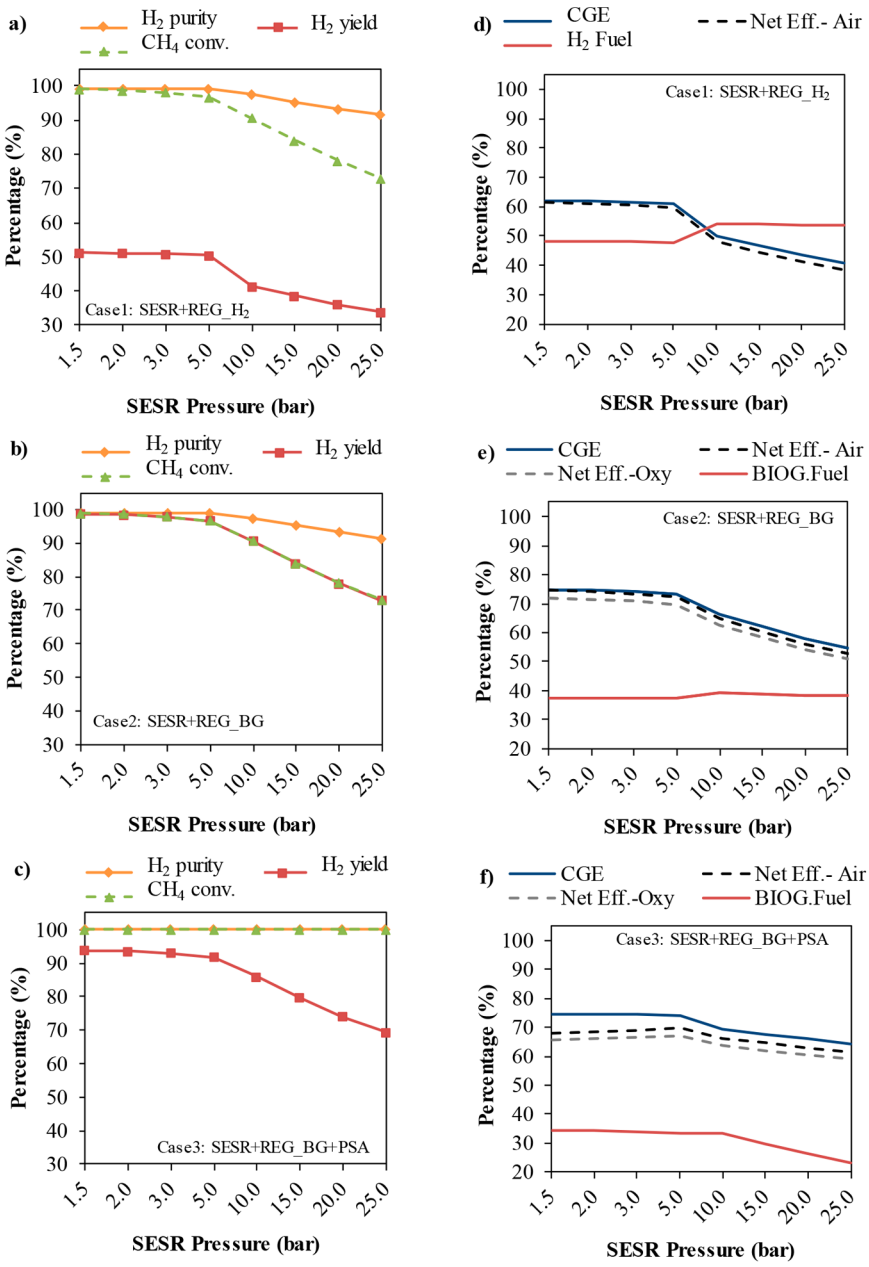

Figure 6. Effect of SESR pressure on H_2 purity, H_2 yield, and CH_4 conversion (a−c) and on cold gas efficiency (CGE), net efficiency (NE, using both air, Net Eff. A, and oxy-combustion, Net Eff-B, in REG), and fuel consumption for sorbent regeneration (d−f) for the different process configurations studied: (a, d) use of a fraction of the produced hydrogen as fuel for sorbent regeneration (SESR+REG_H_2), (b, e) use of biogas as fuel for sorbent regeneration (SESR+REG_BG), and (c, f) addition of a PSA unit and use of biogas and off-gas (PSA-OG) for sorbent regeneration (SESR+REG_BG+PSA). SESR conditions: S/CH_4 = 5.5, T = 600 °C, biogas = 60/40 vol % CH_4/CO_2, and 50% sorbent excess.

PEMFC), where the CO content in the H_2 stream is critical, another way to achieve lower CO concentrations could be to use higher operating pressures.[53] Therefore, the process layout proposed in Case 3 could be interesting when producing H_2 for fuel cell applications, since H_2 purity and CH_4 conversion are 100% regardless the process pressure. However, the negative impact of high pressure values on the H_2 yield should be carefully considered.

Figure 6d−f shows that CGE and NE follow a similar trend to H_2 yield. CGE decreases as pressure increases following the decrease in methane conversion and, hence, in hydrogen production. In Cases 1 and 2 (Figure 6d and 6e), CGE and NE values when air combustion is used in REG are close at low SESR pressures (1.5−5 bar) due to the lower workload required for the compression. At higher operating pressures (5−25 bar), NE for combustion in air is 1.5% to 2.3% lower than CGE as a consequence of the increase in the workload of the auxiliaries with process pressure. In Case 3 (Figure 6f), the PSA unit has an apparent impact on the net efficiency of the whole process. When air is used in REG, NE lowers from 6.8% to 4.4% below CGE in the pressure range of 1.5−5 bar and 3% at higher pressures. The impact of the PSA is more noticeable at low pressures because the gap between the process and PSA pressure is higher, requiring much more work in the compressor to match both pressures upstream of the SESR unit. The slight increase in NE between 1.5 and 5 bar responds

https://doi.org/10.1021/acssuschemeng.2c07316
ACS Sustainable Chem. Eng. 2023, 11, 4759−4775

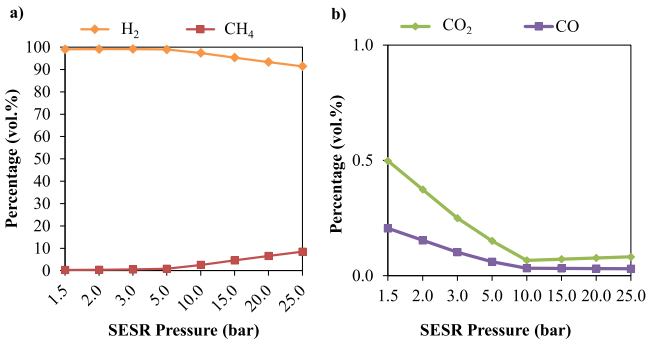

Figure 7. Effect of SESR pressure on H_2 and CH_4 concentrations (a) and CO_2 and CO concentrations (b) in the gas coming out from the SESR reactor. SESR conditions: S/CH_4 = 5.5, T = 600 °C, biogas = 60/40 vol % CH_4/CO_2, and 50% sorbent excess.

to the slightly lower gap as pressure increases. In Case 3, fuel consumption decreases when pressure increases above 5 bar. A higher content of CH_4 in PSA-OG and, hence, a higher calorific value of the off-gas reduces the amount of biogas required as fuel for sorbent regeneration. In the cases using biogas as fuel, a lower value (2.4%) of NE when using oxy-combustion in REG is explained by the penalty of the ASU.

For pressures above 5 bar, the formation of $Ca(OH)_2$ is observed under simulation conditions (Table 7). As reported

Table 7. Effect of SESR Pressure on Composition of Solids Circulating between SESR and REG[a]

	Solids composition at SESR outlet (%)		
SESR pressure (bar)	$CaCO_3$	CaO	$Ca(OH)_2$
1.5	65.1	34.9	0.0
2	65.3	34.7	0.0
3	65.3	34.7	0.0
5	65.0	35.0	0.0
10	62.7	0.0	37.3
15	60.1	0.0	39.9
20	57.7	0.0	42.3
25	55.7	0.0	44.3

[a]SESR conditions: S/CH_4 = 5.5, T = 600 °C, biogas = 60/40 vol % CH_4/CO_2, and 50% sorbent excess.

above (see the Effect of SESR Reactor Temperature section), there is a marked change in the analyzed variables between 5 and 10 bar in Figure 9, which is explained by the formation of $Ca(OH)_2$. When $Ca(OH)_2$ is formed, more heat for regeneration is needed, decreasing the efficiency of the process and increasing the fuel needed in the REG reactor. As explained above, the effect of $Ca(OH)_2$ formation is more pronounced when the hydrogen-rich stream is used as fuel (Figure 6a) than when using biogas (Figure 6e and f) because the heating value of biogas is higher than that of hydrogen.

The amount of energy recovered from the SESR reactor (see Table S2 of the Supporting Information) is 2.0 MW in the 1.5 to 5 bar pressure range. As pressure increases from 5 to 25 bar, the energy recovered increases from 2.0 to 3.7 MW. As the SESR pressure increases, the methane conversion during SESR decreases, and less heat is consumed by the reforming reaction, so there is more heat released by carbonation available for recovery.

Effect of Steam to Methane (S/CH_4) Ratio. Steam is usually fed beyond its stoichiometric limit to promote hydrogen productivity and prevent coking.[56] Therefore, a wide range of S/CH_4 ratios (3−6.5) has been studied. The effects of the S/CH_4 ratio on H_2 purity, CH_4 conversion, and H_2 yield for the different process configurations are shown in Figure 8a−c. For Cases 1 and 2, H_2 purity increases up to 97.9 vol % for S/CH_4 between 3 and 5 (Figure 8a and b), followed by a slight decrease, and finally increases up to 98.3 vol % at a S/CH_4 ratio of 6.5. In Case 3, H_2 purity reaches a value of 100% for all S/CH_4 ratios (Figure 8c) due to the PSA unit purifying H_2. The effect of the S/CH_4 ratio on the H_2 purity is in agreement with the literature since higher CH_4 conversion leads to higher H_2 production and less off-gas methane contaminant content.[57]

CH_4 conversion also increases with the S/CH_4 ratio since higher amounts of steam favor both steam reforming (eq 2) and water−gas shift (eq 3) reactions.[56] In Cases 1 and 2, CH_4 conversion increases from 76.5% to 94.0% as the S/CH_4 ratio increases from 3 to 6.5. However, for Case 3, CH_4 conversion reaches a value of 100% for all S/CH_4 ratios because the recycle of PSA-OG allows burning the unreacted CH_4 from SESR in the REG reactor. Therefore, by increasing the S/CH_4 ratio, the CH_4 conversion significantly increases because the excess steam shifts the reforming equilibrium toward a higher feedstock conversion.

On the other hand, H_2 yield increases with the S/CH_4 ratio in Cases 2 and 3 (Figure 8b and c). In Case 2, it shows higher values, increasing from 76.5% to 94.0% in the 3−6.5 S/CH_4 ratio range, while in Case 3, it increases from 72.6% to 89.3% as the S/CH_4 ratio increases from 3 to 6.5. This lower value in Case 3 is explained because a small fraction of the H_2 produced is burned while recycling PSA-OG to the REG reactor due to the assumption of 95% separation efficiency of the PSA unit. However, in Case 1 (Figure 8a), H_2 yield is lower than in the other two configurations due to hydrogen consumption in REG, as already explained. Its value is around 50% for S/CH_4 ratios between 3 and 5, and it notably decreases to 39.8% for higher S/CH_4 values due to $Ca(OH)_2$ formation (Table 8). This effect, as explained above, is stronger in the case of using H_2 for sorbent regeneration (as compared to biogas) since hydrogen has a lower heating value, and hence, a higher amount of fuel is needed.

The effect of the S/CH_4 molar ratio on the SESR reactor outlet gas composition is shown in Figure 9. Higher S/CH_4 molar ratios increase the H_2 concentration while reducing the CH_4 content (Figure 9a), as it has been previously reported in the literature.[19] On the other hand, the CO_2 and CO concentrations remain almost unchanged for the S/CH_4 range evaluated (Figure 9b), indicating that carbonation proceeds satisfactorily, from a thermodynamic point of view, in an atmosphere with steam excess.

The results corresponding to CGE and NE, as well as fuel consumption for sorbent regeneration, are shown in Figure 8d−f. The effect of the $Ca(OH)_2$ formation is also apparent in those plots since it forms at S/CH_4 ratios higher than 5.25 (Table 8). The lowest fuel consumption in REG is achieved when a PSA unit is added to the process due to the PSA-OG recycling, i.e., Case 3 (Figure 8f), which corresponds to the highest process efficiencies of the three studied designs. It should be highlighted that the heat content of PSA-OG can reduce significantly the fuel consumption at low S/CH_4 ratios. In Case 3, CGE decreases from 76.5% to 74.4% as S/CH_4 increases from 3 to 5, then to 68.3% at a S/CH_4 ratio of 6.5. When using a lower S/CH_4 ratio, the content of CH_4 in the

https://doi.org/10.1021/acssuschemeng.2c07316
ACS Sustainable Chem. Eng. 2023, 11, 4759−4775

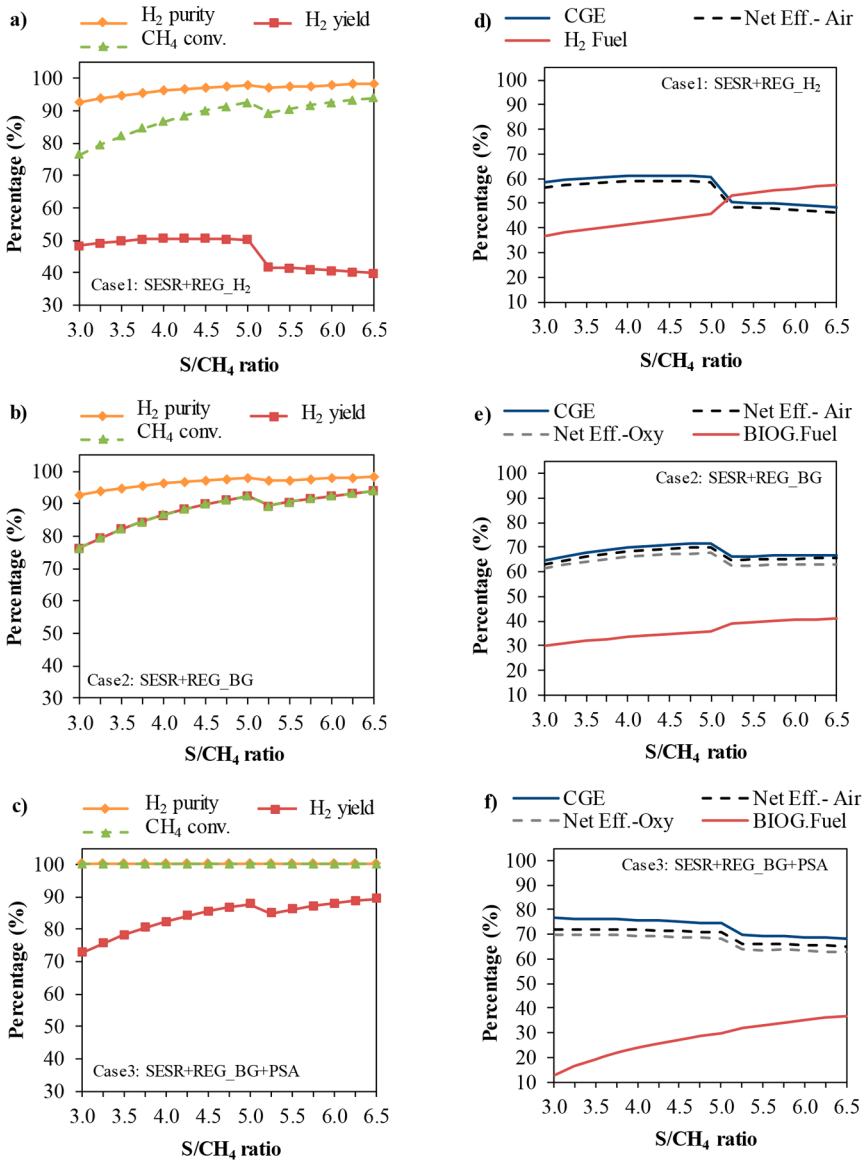

Figure 8. Effect of S/CH_4 on H_2 purity, H_2 yield, and CH_4 conversion (a–c) and on cold gas efficiency (CGE), net efficiency (NE, using both air, Net Eff. A, and oxy-combustion, Net Eff-B, in REG), and fuel consumption for sorbent regeneration (d–f) for the different process configurations studied: (a, d) use of a fraction of the produced hydrogen as fuel for sorbent regeneration (SESR+REG_H_2), (b, e) use of biogas as fuel for sorbent regeneration (SESR+REG_BG), and (c, f) addition of a PSA unit and use of biogas and off-gas (PSA-OG) for sorbent regeneration (SESR +REG_BG+PSA). SESR conditions: 600 °C, P = 10 bar, biogas = 60/40 vol % CH_4/CO_2, and 50% sorbent excess.

Table 8. Effect of S/CH_4 on Composition of Solids Circulating between SESR and REG[a]

	Solids composition at SESR outlet (%)		
S/CH_4 ratio	$CaCO_3$	CaO	$Ca(OH)_2$
3.00	57.1	42.9	0.0
3.50	59.4	40.6	0.0
4.00	61.2	38.8	0.0
4.50	62.5	37.5	0.0
5.00	63.5	36.5	0.0
5.25	62.3	0.0	37.7
5.50	62.7	0.0	37.3
6.00	63.5	0.0	36.5
6.50	64.1	0.0	35.9

[a]SESR conditions: 600 °C, P = 10 bar, biogas = 60/40 vol % CH_4/CO_2, and 50% sorbent excess.

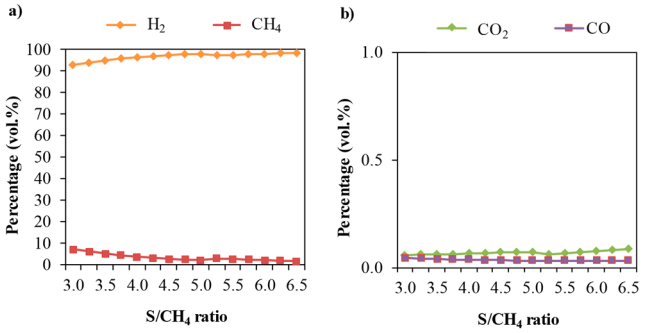

Figure 9. Effect of S/CH_4 on H_2 and CH_4 concentrations (a) and CO_2 and CO concentrations (b) in the gas coming out from the SESR reactor. SESR conditions: 600 °C, P = 10 bar, biogas = 60/40 vol % CH_4/CO_2, and 50% sorbent excess.

https://doi.org/10.1021/acssuschemeng.2c07316
ACS Sustainable Chem. Eng. 2023, 11, 4759−4775

Table 9. Optimal Operating Conditions with Maximum H_2 Purity for Biogas SESR Configurations Evaluated[a]

Case No.	T (°C)	P (bar)	S/CH_4	H_2 purity (vol %)	CH_4 conversion (%)	H_2 yield (%)	CGE (%)	NE (%)	CO_2 capture efficiency (%)	Potential CO_2 capture efficiency in case of indirect heating (%)
Case 1-Air	625	5	5	98.5	95.8	53.8	65.1	63.5	98.0 (zero)	96.5 (negative)
Case 2-Air	625	5	5	98.5	95.8	95.6	75.7	74.5	97.7 (zero)	63.1 (negative)
Case 2-Oxy	625	5	5	98.5	95.8	95.6	75.7	72.0	98.9 (negative)	–
Case 3-Air	675	5	5	100	100	90.8	77.3	72.5	100 (zero)	66.1 (negative)
Case 3-Oxy	675	5	5	100	100	90.8	77.3	70.2	100 (negative)	–

[a]SESR conditions: biogas = 60/40 vol % CH_4/CO_2, and 50% sorbent excess.

PSA-OG is higher, due to the lower methane conversion in SESR, which decreases the consumption of biogas for regeneration, implying a positive impact in the CGE for lower S/CH_4 values. CGE has lower values in Cases 1 and 2 than in Case 3. In Case 1, CGE increases from 58.4% to 60.7% for S/CH_4 values between 3 and 5 according to the higher methane conversion but then decreases to 48.2% at a S/CH_4 ratio of 6.5. In Case 2, CGE decreases from 64.6% to 71.6% as S/CH_4 increases from 3 to 5, then to 66.9% at S/CH_4 ratio of 6.5. In Cases 1 and 2, when using air in REG, NE is 1.5%−2.2% lower than CGE, whereas when oxy-combustion is used in REG, NE reduces an additional 2.2% in Case 2 due to the ASU penalty. In Case 3, when using air in REG, NE is 3.1%−4.4% lower than CGE, whereas when oxy-combustion is used in REG, NE reduces an additional 2.4% due to the ASU penalty.

The amount of energy recovered from the SESR reactor is 2.1 MW when the S/CH_4 ratio is lower than 5, while it grows to 3.4 MW when S/CH_4 is higher than 5.25 (see Table S3 of the Supporting Information). The increase in heat recovery can be ascribed to the heat released upon the formation of $Ca(OH)_2$ at higher S/CH_4 ratios, according to eq 13.

Discussion of SESR Configurations to Optimize H_2 Purity and CO_2 Capture. After evaluating five case studies from the three different process configurations for the SESR of biogas proposed, the optimal operating conditions to reach maximum H_2 purity according to the sensitivity analysis are shown in Table 9. For optimization purposes, the optimal conditions have been selected considering the avoidance of $Ca(OH)_2$ formation and the recovery of waste heat available in the outlet CO_2 stream (assuming 10% of heat losses as in the heat recovered from the SESR reactor). The formation of $Ca(OH)_2$ would not only result in higher energy consumption in the calciner, decreasing the overall efficiency, but also in an extra steam consumption that decreases steam excess and could favor coke deposition in the catalyst surface. The CO_2 capture efficiency is also determined for each configuration. It should be highlighted that the optimal conditions given by this thermodynamic study are in good agreement with those reported in previous experimental works on biogas SESR.[18,19] Under the optimal conditions, the experimental results are very close to those predicted by the thermodynamic equilibrium because the solid sorbent removes separation efficiency in situ CO_2 from the gas phase and shifts the reforming reaction equilibrium toward product formation, increasing the conversion.

The differences between air or oxy-fuel combustion in REG can be seen in the net efficiency and CO_2 capture for Cases 2 and 3. Case 1 is only evaluated in air combustion REG. For Cases 1 and 2, the CO_2 capture efficiency is ∼98% or even above, while in Case 3, the PSA unit boosts the CO_2 capture efficiency to ∼100%. The CO_2 capture using air for regeneration means global zero emissions for the process since, even though we are feeding a renewable feedstock such as biogas, the outlet CO_2 stream is diluted with the N_2 from the air. However, in oxy-fuel combustion conditions for sorbent regeneration, the CO_2 capture translates into negative emissions from the process since in these cases a pure outlet CO_2 stream is obtained.

It would however be possible to reach negative emissions using air combustion for sorbent regeneration if the calciner reactor was indirectly heated. Indirect heating can be achieved by supplying energy to the calciner from an external combustor via a fluidized-bed heat exchanger[5,39] or using heat pipes,[40−42] as recently reported in the literature.[30] The negative emissions that could be reached with indirect heating for the studied cases are shown in Table 9. As it can be seen, comparing Cases 1 and 2, a higher efficiency of the process is reached when biogas is used as fuel for sorbent regeneration in REG (Case 2) compared to H_2 (Case 1). In Case 2, NE is 74.5% when using air and 72.0% when using oxy-fuel combustion, alongside H_2 purity of 98.5 vol %, CH_4 conversion of 95.8%, and H_2 yield of 95.6% operating at 625 °C, 5 bar, and S/CH_4 = 5. In this case, zero carbon emissions are achieved if air is used in REG, while negative emissions with CO_2 capture efficiency of 98.9% are reached for oxy-fuel combustion.

In Case 3, biogas is used for sorbent regeneration combined with a PSA unit at the end. Its NE is 72.5% when using air and 70.2% when using oxy-fuel combustion, i.e., 2% and 1.8% points lower than that in Case 2. However, H_2 purity and CH_4 conversion reach nearly 100%, with H_2 yield of 90.8%, when operating at 675 °C, 5 bar, and S/CH_4 = 5. In this case, zero carbon emissions are achieved if air is used in REG, while negative emissions with CO_2 capture efficiency of ∼100% are reached for oxy-fuel combustion. Therefore, assuming a slightly lower net efficiency by incorporating a PSA unit into the system, Case 3 produces a high-purity H_2 that meets the high requirements of, for example, fuel cells, under both air and oxy-fuel combustion conditions.

In summary, biogas SESR with sorbent regeneration using biogas (SESR+REG_BG) (Case 2) could be the best option if a H_2 purity of 98.5 vol % fulfils the hydrogen requirements needed (with a CGE of 75.7%). For this configuration, oxy-fuel combustion sorbent regeneration delivers negative emissions with CO_2 capture efficiency of 98.9%, whereas indirect air firing would lower the CO_2 capture efficiency to 63.1% but preserve the negative emission. On the other hand, the addition of a PSA unit to the biogas SESR system that also uses biogas for sorbent regeneration (SESR+REG_BG+PSA) (Case 3) is needed if a H_2 purity of nearly 100 vol % is required (with a CGE of 77.3%). Additionally, negative CO_2 capture

https://doi.org/10.1021/acssuschemeng.2c07316
ACS Sustainable Chem. Eng. 2023, 11, 4759−4775

efficiency of ∼100% could be reached in oxy-fuel combustion atmosphere or 66.1% in indirect air heating for the calciner.

CONCLUSIONS

This work proposes a novel process to produce renewable high-purity hydrogen from biogas with low-carbon emissions using the SESR technology. Three different process configurations and five case studies have been evaluated using a thermodynamic analysis performed in Aspen Plus to optimize the heat integration of the system, while maximizing the hydrogen production, energy efficiency, and CO_2 capture. A heat exchanger network (HEN) has been designed to recover as much heat as possible from the system. From a parametric analysis, the effects of the operating process conditions on the process performance were studied through the H_2 purity, H_2 yield, CH_4 conversion, energy efficiency, fuel consumption for the sorbent regeneration step, and CO_2 capture.

The results show that the H_2 purity keeps constant for all biogas compositions (50−80 vol % CH_4, balance CO_2). The SESR+REG_BG configuration, using biogas to meet the energy requirements of the sorbent regeneration, delivers a H_2 purity of 98.5 vol % at 625 °C, 5 bar and S/CH_4 = 5, with a CGE of 75.7%, and zero carbon emissions in air regeneration operation. A CO_2 capture efficiency of 98.9% can be achieved in oxy-fuel combustion sorbent regeneration, and the emissions are labeled negative. The SESR+REG_H_2 configuration, where part of the H_2 produced by the system is used to heat the calciner reactor, can produce H_2 purity of 98.5 vol % at 625 °C, 5 bar, and S/CH_4 = 5, but with lower efficiency (CGE = 65.1%) than that in the biogas case. Finally, the SESR +REG_BG+PSA configuration can produce ∼100% H_2 purity at 675 °C, 5 bar, and S/CH_4 = 5, with a CGE of 77.3% and zero carbon emissions if an air-fired calciner is applied. However, negative emissions and ∼100% CO_2 capture efficiency are feasible if regeneration is performed in an oxy-fuel combustion atmosphere. The use of oxy-fuel combustion in the regeneration stage gives a penalty of 2.3% points in the net efficiency of the process, although it enables a process with negative carbon emissions. The results of this equilibrium study demonstrate the thermodynamic feasibility of the SESR process of biogas and provide the optimal process configurations and operating conditions to maximize the cold gas efficiency of the process. Even though it is outside of the scope of this study, the outcome of this work lays the foundation for subsequent dynamic modeling to design the reactors and heat recovery systems needed to scale up the biogas SESR process.

ASSOCIATED CONTENT

Supporting Information

The Supporting Information is available free of charge at https://pubs.acs.org/doi/10.1021/acssuschemeng.2c07316.

Aspen Plus flowsheets of renewable hydrogen production from biogas SESR for the different process configurations studied (PDF)

AUTHOR INFORMATION

Corresponding Authors

Covadonga Pevida − *Instituto de Ciencia y Tecnología del Carbono, INCAR-CSIC, 33011 Oviedo, Spain;* orcid.org/0000-0002-4662-8448; Email: cpevida@incar.csic.es

María Victoria Gil − *Instituto de Ciencia y Tecnología del Carbono, INCAR-CSIC, 33011 Oviedo, Spain;* orcid.org/0000-0002-2258-3011; Email: victoria.gil@incar.csic.es

Authors

Alma Capa − *Instituto de Ciencia y Tecnología del Carbono, INCAR-CSIC, 33011 Oviedo, Spain; Energy and Sustainability Theme, Cranfield University, Cranfield, Bedfordshire MK43 0AL, United Kingdom*

Yongliang Yan − *Materials, Concept and Reaction Engineering (MatCoRE) Group, School of Engineering, Newcastle University, Newcastle Upon Tyne NE1 7RU, United Kingdom*

Fernando Rubiera − *Instituto de Ciencia y Tecnología del Carbono, INCAR-CSIC, 33011 Oviedo, Spain;* orcid.org/0000-0003-0385-1102

Peter T. Clough − *Energy and Sustainability Theme, Cranfield University, Cranfield, Bedfordshire MK43 0AL, United Kingdom;* orcid.org/0000-0003-1820-0484

Complete contact information is available at: https://pubs.acs.org/10.1021/acssuschemeng.2c07316

Author Contributions

The manuscript was written through contributions of all authors. All authors have given approval to the final version of the manuscript.

Notes

The authors declare no competing financial interest.

ACKNOWLEDGMENTS

This work was carried out with financial support from the Spanish MICINN through Grant PID2020-119539RB-I00, funded by MCIN/AEI/10.13039/501100011033, and from the Gobierno del Principado de Asturias (PCTI, ref. IDI/2021/000060). P.T.C. would like to thank the UK Department for Business, Energy and Industrial Strategy for supporting research into this area through the Bio-HyPER project funded by the H_2 BECCS Phase 1 competition (H2BECCS107). A.C. acknowledges a fellowship awarded by the Spanish MICINN FPI program through Grant PRE2018-083634, funded by MCIN/AEI/10.13039/501100011033 and by "ESF Investing in your future". M.V.G. acknowledges support from the Spanish AEI through the Ramón y Cajal Grant RYC-2017-21937 funded by MCIN/AEI/10.13039/501100011033 and by "ESF Investing in your future".

REFERENCES

(1) El-Emam, R. S.; Özcan, H. Comprehensive Review on the Techno-Economics of Sustainable Large-Scale Clean Hydrogen Production. *Journal of Cleaner Production* **2019**, *220*, 593−609.

(2) Minh, D. P.; Siang, T. J.; Vo, D. V. N.; Phan, T. S.; Ridart, C.; Nzihou, A.; Grouset, D. *Hydrogen Production from Biogas Reforming: An Overview of Steam Reforming, Dry Reforming, Dual Reforming, and Tri-Reforming of Methane*; Elsevier Ltd., 2018. DOI: 10.1016/B978-0-12-811197-0.00004-X.

(3) *Global Hydrogen Review 2021*; International Energy Agency, 2021. DOI: 10.1787/39351842-en.

(4) Abdin, Z.; Zafaranloo, A.; Rafiee, A.; Mérida, W.; Lipiński, W.; Khalilpour, K. R. Hydrogen as an Energy Vector. *Renewable and Sustainable Energy Reviews* **2020**, *120*, 109620.

(5) Stenberg, V.; Spallina, V.; Mattisson, T.; Rydén, M. Techno-Economic Analysis of H2 Production Processes Using Fluidized Bed Heat Exchangers with Steam Reforming − Part 1: Oxygen Carrier

Aided Combustion. *Int. J. Hydrogen Energy* **2020**, *45* (11), 6059−6081.
(6) Di Giuliano, A.; Gallucci, K. Sorption Enhanced Steam Methane Reforming Based on Nickel and Calcium Looping: A Review. *Chemical Engineering and Processing - Process Intensification.* **2018**, *130*, 240.
(7) Cherbanski, R.; Molga, E. Sorption-Enhanced Steam Methane Reforming (SE-SMR) − A Review: Reactor Types, Catalyst and Sorbent Characterization, Process Modeling. *Chem. Process Eng. - Inz. Chem. i Proces.* **2018**, *39* (4), 427−448.
(8) Xu, Y.; Lu, B.; Luo, C.; Chen, J.; Zhang, Z.; Zhang, L. Sorption Enhanced Steam Reforming of Ethanol over Ni-Based Catalyst Coupling with High-Performance CaO Pellets. *Chem. Eng. J.* **2021**, *406*, 126903.
(9) Saupsor, J.; Kasempremchit, N.; Bumroongsakulsawat, P.; Kim-Lohsoontorn, P.; Wongsakulphasatch, S.; Kiatkittipong, W.; Laosiripojana, N.; Gong, J.; Assabumrungrat, S. Performance Comparison among Different Multifunctional Reactors Operated under Energy Self-Sufficiency for Sustainable Hydrogen Production from Ethanol. *Int. J. Hydrogen Energy* **2020**, *45* (36), 18309−18320.
(10) Wang, N.; Feng, Y.; Chen, Y.; Guo, X. Lithium-Based Sorbent from Rice Husk Materials for Hydrogen Production via Sorption-Enhanced Steam Reforming of Ethanol. *Fuel* **2019**, *245*, 263−273.
(11) Fermoso, J.; He, L.; Chen, D. Production of High Purity Hydrogen by Sorption Enhanced Steam Reforming of Crude Glycerol. *Int. J. Hydrogen Energy* **2012**, *37* (19), 14047−14054.
(12) Shokrollahi Yancheshmeh, M.; Radfarnia, H. R.; Iliuta, M. C. Sustainable Production of High-Purity Hydrogen by Sorption Enhanced Steam Reforming of Glycerol over CeO_2-Promoted $Ca_9Al_6O_{18}$-CaO/NiO Bifunctional Material. *ACS Sustain. Chem. Eng.* **2017**, *5* (11), 9774−9786.
(13) Shokrollahi Yancheshmeh, M.; Iliuta, M. C. Embedding Ni in Ni-Al Mixed-Metal Alkoxide for the Synthesis of Efficient Coking Resistant Ni-CaO-Based Catalyst-Sorbent Bifunctional Materials for Sorption-Enhanced Steam Reforming of Glycerol. *ACS Sustain. Chem. Eng.* **2020**, *8* (45), 16746−16756.
(14) Esteban-Díez, G.; Gil, M. V.; Pevida, C.; Chen, D.; Rubiera, F. Effect of Operating Conditions on the Sorption Enhanced Steam Reforming of Blends of Acetic Acid and Acetone as Bio-Oil Model Compounds. *Appl. Energy* **2016**, *177*, 579−590.
(15) Fermoso, J.; Gil, M. V.; Rubiera, F.; Chen, D. Multifunctional Pd/Ni-Co Catalyst for Hydrogen Production by Chemical Looping Coupled with Steam Reforming of Acetic Acid. *ChemSusChem* **2014**, *7* (11), 3063−3077.
(16) Gil, M. V.; Fermoso, J.; Rubiera, F.; Chen, D. H_2 Production by Sorption Enhanced Steam Reforming of Biomass-Derived Bio-Oil in a Fluidized Bed Reactor: An Assessment of the Effect of Operation Variables Using Response Surface Methodology. *Catal. Today* **2015**, *242*, 19−34.
(17) Gil, M. V.; Rout, K. R.; Chen, D. Production of High Pressure Pure H_2 by Pressure Swing Sorption Enhanced Steam Reforming (PSSESR) of Byproducts in Biorefinery. *Appl. Energy* **2018**, *222*, 595.
(18) Capa, A.; García, R.; Chen, D.; Rubiera, F.; Pevida, C.; Gil, M. V. On the Effect of Biogas Composition on the H2 Production by Sorption Enhanced Steam Reforming (SESR). *Renew. Energy* **2020**, *160*, 575−583.
(19) García, R.; Gil, M. V.; Rubiera, F.; Chen, D.; Pevida, C. Renewable Hydrogen Production from Biogas by Sorption Enhanced Steam Reforming (SESR): A Parametric Study. *Energy* **2021**, *218*, 119491.
(20) Alves, H. J.; Bley Junior, C.; Niklevicz, R. R.; Frigo, E. P.; Frigo, M. S.; Coimbra-Araújo, C. H. Overview of Hydrogen Production Technologies from Biogas and the Applications in Fuel Cells. *Int. J. Hydrogen Energy* **2013**, *38* (13), 5215−5225.
(21) Yang, L.; Ge, X.; Wan, C.; Yu, F.; Li, Y. Progress and Perspectives in Converting Biogas to Transportation Fuels. *Renew. Sustain. Energy Rev.* **2014**, *40*, 1133−1152.
(22) Fontaine, D.; Eriksen, J.; Sørensen, P. Sulfur from Biogas Desulfurization: Fate of S during Storage in Manure and after Application to Plants. *Sci. Total Environ.* **2021**, *754*, 142180.
(23) Kong, F.; Swift, J.; Zhang, Q.; Fan, L. S.; Tong, A. Biogas to H_2 Conversion with CO_2 Capture Using Chemical Looping Technology: Process Simulation and Comparison to Conventional Reforming Processes. *Fuel* **2020**, *279*, 118479.
(24) Gao, Y.; Jiang, J.; Meng, Y.; Yan, F.; Aihemaiti, A. A Review of Recent Developments in Hydrogen Production via Biogas Dry Reforming. *Energy Convers. Manag.* **2018**, *171*, 133−155.
(25) Yentekakis, I. V.; Goula, G. Biogas Management: Advanced Utilization for Production of Renewable Energy and Added-Value Chemicals. *Front. Environ. Sci.* **2017**, *5*, na DOI: 10.3389/fenvs.2017.00007.
(26) Masoudi Soltani, S.; Lahiri, A.; Bahzad, H.; Clough, P.; Gorbounov, M.; Yan, Y. Sorption-Enhanced Steam Methane Reforming for Combined CO_2 Capture and Hydrogen Production: A State-of-the-Art Review. *Carbon Capture Sci. Technol.* **2021**, *1*, No. 100003.
(27) Tian, X.; Wang, S.; Zhou, J.; Xiang, Y.; Zhang, F.; Lin, B.; Liu, S.; Luo, Z. Simulation and Exergetic Evaluation of Hydrogen Production from Sorption Enhanced and Conventional Steam Reforming of Acetic Acid. *Int. J. Hydrogen Energy* **2016**, *41* (46), 21099−21108.
(28) Tzanetis, K. F.; Martavaltzi, C. S.; Lemonidou, A. A. Comparative Exergy Analysis of Sorption Enhanced and Conventional Methane Steam Reforming. *Int. J. Hydrogen Energy* **2012**, *37* (21), 16308−16320.
(29) Alam, S.; Kumar, J. P.; Rani, K. Y.; Sumana, C. Self-Sustained Process Scheme for High Purity Hydrogen Production Using Sorption Enhanced Steam Methane Reforming Coupled with Chemical Looping Combustion. *J. Clean. Prod.* **2017**, *162*, 687−701.
(30) Yan, Y.; Thanganadar, D.; Clough, P. T.; Mukherjee, S.; Patchigolla, K.; Manovic, V.; Anthony, E. J. Process Simulations of Blue Hydrogen Production by Upgraded Sorption Enhanced Steam Methane Reforming (SE-SMR) Processes. *Energy Convers. Manag.* **2020**, *222*, 113144.
(31) Antzara, A.; Heracleous, E.; Bukur, D. B.; Lemonidou, A. A. Thermodynamic Analysis of Hydrogen Production via Chemical Looping Steam Methane Reforming Coupled with in Situ CO_2 Capture. In. *Energy Procedia* **2014**, *63*, 6576.
(32) Phuluanglue, A.; Khaodee, W.; Assabumrungrat, S. Simulation of Intensified Process of Sorption Enhanced Chemical-Looping Reforming of Methane: Comparison with Conventional Processes. *Comput. Chem. Eng.* **2017**, *105*, 237−245.
(33) Ebneyamini, A.; Grace, J. R.; Lim, C. J.; Ellis, N.; Elnashaie, S. S. E. H. Simulation of Limestone Calcination for Calcium Looping: Potential for Autothermal and Hydrogen-Producing Sorbent Regeneration. *Ind. Eng. Chem. Res.* **2019**, *58*, 8636.
(34) Antzara, A.; Heracleous, E.; Bukur, D. B.; Lemonidou, A. A. Thermodynamic Analysis of Hydrogen Production via Chemical Looping Steam Methane Reforming Coupled with in Situ CO2 Capture. *Int. J. Greenh. Gas Control* **2015**, *32*, 115−128.
(35) Barelli, L. Ã.; Bidini, G.; Corradetti, A.; Desideri, U. Study of the Carbonation − Calcination Reaction Applied to the Hydrogen Production from Syngas. *Energy* **2007**, *32*, 697−710.
(36) Barelli, L.; Bidini, G.; Corradetti, A.; Desideri, U. Production of Hydrogen through the Carbonation-Calcination Reaction Applied to CH_4/CO_2 Mixtures. *Energy* **2007**, *32* (5), 834−843.
(37) Capa, A.; García, R.; Rubiera, F.; Pevida, C.; Gil, M. V. Energy Analysis on the Effect of Biogas Composition in the Sorption Enhanced Steam Reforming (SESR) for Green Hydrogen Production. In *29th European Biomass Conference and Exhibition*, 2021; pp 1366−1370.
(38) Marín, P.; Díez, F. V.; Ordóñez, S. Reverse Flow Reactors as Sustainable Devices for Performing Exothermic Reactions: Applications and Engineering Aspects. *Chemical Engineering and Processing - Process Intensification* **2019**, *135*, 175−189.

(39) Stenberg, V.; Rydén, M.; Mattisson, T.; Lyngfelt, A. Exploring Novel Hydrogen Production Processes by Integration of Steam Methane Reforming with Chemical-Looping Combustion (CLC-SMR) and Oxygen Carrier Aided Combustion (OCAC-SMR). *Int. J. Greenh. Gas Control* **2018**, *74*, 28−39.
(40) Junk, M.; Reitz, M.; Strohle, J.; Epple, B. Technical and Economical Assessment of the Indirectly Heated Carbonate Looping Process. *J. Energy Resour. Technol. Trans. ASME* **2016**, *138* (4), 1−8.
(41) Hoeftberger, D.; Karl, J. The Indirectly Heated Carbonate Looping Process for CO_2 Capture A Concept with Heat Pipe Heat Exchanger. *J. Energy Resour. Technol. Trans. ASME* **2016**, *138* (4), 1−7.
(42) Reitz, M.; Junk, M.; Ströhle, J.; Epple, B. Design and Operation of a 300 KWth Indirectly Heated Carbonate Looping Pilot Plant. *Int. J. Greenh. Gas Control* **2016**, *54*, 272−281.
(43) Rydén, M.; Ramos, P. H2 Production with CO2 Capture by Sorption Enhanced Chemical-Looping Reforming Using NiO as Oxygen Carrier and CaO as CO2 Sorbent. *Fuel Process. Technol.* **2012**, *96* (0), 27−36.
(44) Kavosh, M.; Patchigolla, K.; Anthony, E. J.; Oakey, J. E. Carbonation Performance of Lime for Cyclic CO_2 Capture Following Limestone Calcination in Steam/CO_2 Atmosphere. *Appl. Energy* **2014**, *131*, 499−507.
(45) Johnsen, K.; Grace, J. R.; Elnashaie, S. S. E. H.; Kolbeinsen, L.; Eriksen, D. Modeling of Sorption-Enhanced Steam Reforming in a Dual Fluidized Bubbling Bed Reactor. *Ind. Eng. Chem. Res.* **2006**, *45* (12), 4133−4144.
(46) Shokrollahi Yancheshmeh, M.; Radfarnia, H. R.; Iliuta, M. C. High Temperature CO2 Sorbents and Their Application for Hydrogen Production by Sorption Enhanced Steam Reforming Process. *Chem. Eng. J.* **2016**, *283*, 420−444.
(47) Dunstan, M. T.; Donat, F.; Bork, A. H.; Grey, C. P.; Müller, C. R. CO_2 Capture at Medium to High Temperature Using Solid Oxide-Based Sorbents: Fundamental Aspects, Mechanistic Insights, and Recent Advances. *Chem. Rev.* **2021**, *121*, 12681.
(48) Broda, M.; Manovic, V.; Imtiaz, Q.; Kierzkowska, A. M.; Anthony, E. J.; Müller, C. R. High-Purity Hydrogen via the Sorption-Enhanced Steam Methane Reforming Reaction over a Synthetic CaO-Based Sorbent and a Ni Catalyst. *Environ. Sci. Technol.* **2013**, *47* (11), 6007−6014.
(49) Di Giuliano, A.; Gallucci, K.; Kazi, S. S.; Giancaterino, F.; Di Carlo, A.; Courson, C.; Meyer, J.; Di Felice, L. Development of Ni- and CaO-Based Mono- and Bi-Functional Catalyst and Sorbent Materials for Sorption Enhanced Steam Methane Reforming: Performance over 200 cycles and Attrition Tests. *Fuel Process. Technol.* **2019**, *195*, 106160.
(50) He, L.; Berntsen, H.; Chen, De Approaching Sustainable H_2 Production: Sorption Enhanced Steam Reforming of Ethanol. *J. Phys. Chem. A* **2010**, *114* (11), 3834−3844.
(51) Anthony, E. J.; Bulewicz, E. M.; Jia, L. Reactivation of Limestone Sorbents in FBC for SO_2 Capture. *Prog. Energy Combust. Sci.* **2007**, *33* (2), 171−210.
(52) Diglio, G.; Hanak, D. P.; Bareschino, P.; Pepe, F.; Montagnaro, F.; Manovic, V. Modelling of Sorption-Enhanced Steam Methane Reforming in a Fixed Bed Reactor Network Integrated with Fuel Cell. *Appl. Energy* **2018**, *210*, 1−15.
(53) Rodríguez, S.; Capa, A.; García, R.; Chen, D.; Rubiera, F.; Pevida, C.; Gil, M. V. Blends of Bio-Oil/Biogas Model Compounds for High-Purity H_2 Production by Sorption Enhanced Steam Reforming (SESR): Experimental Study and Energy Analysis. *Chem. Eng. J.* **2022**, *432*, No. 134396.
(54) Habibi, R.; Pourfayaz, F.; Mehrpooya, M.; Kamali, H. A Natural Gas-Based Eco-Friendly Polygeneration System Including Gas Turbine, Sorption-Enhanced Steam Methane Reforming, Absorption Chiller and Flue Gas CO_2 Capture Unit. *Sustain. Energy Technol. Assessments* **2022**, *52*, 101984.
(55) Zhu, L.; Li, L.; Fan, J. A Modified Process for Overcoming the Drawbacks of Conventional Steam Methane Reforming for Hydrogen Production: Thermodynamic Investigation. *Chem. Eng. Res. Des.* **2015**, *104*, 792−806.
(56) Noor, T.; Gil, M. V.; Chen, D. Production of Fuel-Cell Grade Hydrogen by Sorption Enhanced Water Gas Shift Reaction Using Pd/Ni-Co Catalysts. *Appl. Catal. B Environ.* **2014**, *150−151*, 585.
(57) Ebneyamini, A.; Grace, J. R.; Lim, C. J.; Ellis, N. Simulation of Sorbent-Enhanced Steam Methane Reforming and Limestone Calcination in Dual Turbulent Fluidized Bed Reactors. *Energy Fuel* **2020**, *34*, 7743−7755.

https://doi.org/10.1021/acssuschemeng.2c07316
ACS Sustainable Chem. Eng. 2023, 11, 4759−4775